# Appendix E
# FCT Document Cover Sheet

| | |
|---|---|
| Name/Title of Deliverable/Milestone | Decay Heat Sensitivity Studies for Used BWR Fuel Assemblies |
| Work Package Title and Number | Analysis FT-14OR081001 |
| Work Package WBS Number | 1.02.08.10 |
| Responsible Work Package Manager | John M. Scaglione |
| | (Name/Signature) |

John M. Scaglione

Digitally signed by John M. Scaglione
DN: cn=John M. Scaglione, o=Reactor & Nuclear Systems Division, ou=Used Fuel Systems, email=ScaglioneJM@ornl.gov, c=US
Date: 2014.09.23 17:09:19 -04'00'

Date Submitted 9/23/2014

| Quality Rigor Level for Deliverable/Milestone | ☒ QRL-3 | ☐ QRL-2 | ☐ QRL-1<br>☐ Nuclear Data | ☐ N/A* |
|---|---|---|---|---|

This deliverable was prepared in accordance with ORNL
*(Participant/National Laboratory Name)*

QA program which meets the requirements of
☒ DOE Order 414.1 ☒ NQA-1-2000

**This Deliverable was subjected to:**

☒ Technical Review ☐ Peer Review

**Technical Review (TR)**
**Review Documentation Provided**
☐ Signed TR Report or,
☒ Signed TR Concurrence Sheet or,
☐ Signature of TR Reviewer(s) below

**Peer Review (PR)**
**Review Documentation Provided**
☐ Signed PR Report or,
☐ Signed PR Concurrence Sheet or,
☐ Signature of PR Reviewer(s) below

**Name and Signature of Reviewers**

*Note: In some cases there may be a milestone where an item is being fabricated, maintenance is being performed on a facility, or a document is being issued through a formal document control process where it specifically calls out a formal review of the document. In these cases, documentation (e.g., inspection report, maintenance request, work planning package documentation or the documented review of the issued document through the document control process) of the completion of the activity along with the Document Cover Sheet is sufficient to demonstrate achieving the milestone. QRL for such milestones may be also be marked N/A in the work package provided the work package clearly specifies the requirement to use the Document Cover Sheet and provide supporting documentation.

Publication Tracking System ▸ PTS

# View Record

Close

| | |
|---|---|
| **Pub ID** | 51962 |
| **Title** | Decay Heat Sensitivity Studies for Used BWR Fuel Assemblies |
| **Status** | Submitted for review |
| **Communication Type** | Letter report |
| **ORNL Review?** | Scientific communication that requires ORNL review |
| **Information Category** | Limited By Sponsor |
| **ORNL Report Classification** | |
| **Contact Person** | Mueller, Don |
| **Responsible Organization** | Reactor & Nuclear Systems Division (50159781) |
| **Prepared at** | This scientific communication is being prepared by someone at ORNL. |
| **Authors** | Mueller, Don ORNL (34436)<br>Scaglione, John M. ORNL (939679) |
| **Acknowledgements** | |

**Workflow**

| | | | |
|---|---|---|---|
| 09/12/2014 15:27:35 | Draft | Mueller, Don by Ragle, Katherine L | |
| 09/12/2014 15:28:42 | Author Certification | Mueller, Don | |
| 09/12/2014 15:28:42 | Submitted for review | Mueller, Don | |
| 09/13/2014 11:04:01 | Supervisor | Dunn, Michael E | Approved |
| 09/17/2014 11:12:29 | Technical Reviewer | Radulescu, Georgeta | Recommended |
| 09/19/2014 08:51:52 | Technical Reviewer | Robb, Kevin R | Recommended |
| 09/23/2014 07:13:03 | Technical Editor | Koncinski, Walter S | Recommended |
| 09/23/2014 13:18:00 | Administrative Check | Ragle, Katherine L | Recommended |
| 09/23/2014 15:49:40 | Supervisor | Dunn, Michael E | Approved |
| 09/23/2014 16:38:24 | Program Manager | Scaglione, John M | Approved |
| | *Waiting on the following review(s)* | | |
| | Division Approver | Wagner, John C | |
| | Distributed | Mueller, Don | |

View Comments from Reviewers

| | |
|---|---|
| **Requested Approval Date** | September 19, 2014 |
| **Abstract** | |
| **Report Number** | ORNL/LTR-2014/453 |
| **Secondary ID Number** | FCRD-UFD-2014-000321 |
| **Additional Information** | |
| **User Facility** | Not applicable |
| **Account Number(s)** | 35304A12 |
| **B&R Codes** | AF5865010 |
| **IANs** | |
| **FWPs** | NEAF346 |
| **Overhead Categories** | |
| **Proposal Numbers** | |
| **Keywords** | |

Close

# *Decay Heat Sensitivity Studies for Used BWR Fuel Assemblies*

## Fuel Cycle Research & Development

*Prepared for*
*U.S. Department of Energy*
*Used Fuel Disposition Campaign*

*D.E. Mueller and J.M. Scaglione*
*Oak Ridge National Laboratory*

*September 23, 2014*

**FCRD-UFD-2014-000321**

# SUMMARY

The work reported herein involved investigation of the potential impact of simplifying modeling assumptions and techniques on decay heat values calculated for used boiling water reactor (BWR) nuclear fuel using the SCALE computer code system. Sensitivity studies were performed using realistic BWR fuel assembly designs and by varying reactor depletion conditions and calculation methods. A summary of the results of the sensitivity studies is presented in Table 25. Other than postirradiation decay time, which is the most obvious factor affecting decay heat, modeling of control blade usage, power density, moderator density and initial fuel enrichment may have significant impact on decay heat calculation results. In general terms, reactor condition variations that result in harder (i.e., higher energy) neutron energy spectrum result in higher decay heat values and these effects increase with longer postirradiation decay time periods out to at least 100 years.

Care must be taken in the selection of reactor modeling conditions to avoid excessively high estimation of decay heat. For example, while modeling of control blades fully inserted for the entire in-reactor life-time of an assembly will generate higher decay heat values (i.e., up to 20% higher after 100 years of decay time), such control blade usage never occurs.

This page is intentionally left blank.

# CONTENTS

This page is intentionally left blank.

# FIGURES

This page is intentionally left blank.

# TABLES

This page is intentionally left blank.

# ACRONYMS

| | |
|---|---|
| BWR | boiling water reactor |
| CB | control blade |
| CFR | Code of Federal Regulations |
| DF | Dancoff Factor |
| DH | decay heat |
| HCNGS | Hope Creek Nuclear Generating Station |
| MD | moderator density |
| PD | power density |
| UFD | Used Fuel Disposition |
| UNF | used nuclear fuel |

This page is intentionally left blank.

# USED FUEL DISPOSITION DECAY HEAT SENSITIVITY STUDIES FOR USED BWR FUEL ASSEMBLIES

## 1. INTRODUCTION

The fuel rod clad serves as an important barrier for preventing release of radioactive material from used nuclear fuel (UNF). Analyses of the UNF in transportation and storage systems required by the Code of Federal Regulations (Title 10 CFR Part 71 [1] and Title 10 CFR Part 72 [2]) are performed to ensure that the clad integrity is not compromised under normal and accident conditions.

In simplistic terms, the safety analyses include confirmation that clad temperature and hoop stress limits are not exceeded. One of the primary inputs to the safety analyses is the heat generated by the radioactive decay of the UNF. Radioactive decay heat, which is commonly referred to as "decay heat," affects both the internal gas pressure and temperatures of fuel rods. Generation of defensible decay heat values for use in safety analyses is important. Decay heat varies with reactor operating conditions, fuel assembly design, and postirradiation decay time.

The primary purpose of this report is to present sensitivity-study results that may be used to support the definition of analytical techniques to be used in the generation of decay heat values for boiling water reactor (BWR) UNF.

The sensitivity studies presented in this report were performed using data obtained for fuel stored in Hope Creek Nuclear Generating Station (HCNGS) cask MPC144. The HCNGS data were used because detailed real fuel assembly design and reactor operating data were available. Section 2 provides brief descriptions of the analysis approach, the computational methods, and data used. Descriptions of the HCNGS reactor and fuel are provided in Section 3, along with what are referred to in this report as the "reference results." Numerous sensitivity study results are presented in Section 4. Section 5 provides some observations and conclusions resulting from the sensitivity studies. References are provided in Section 6.

## 2. ANALYSIS METHODS, COMPUTATIONAL METHODS, AND DATA

### 2.1 Analysis Methods

In support of other Used Fuel Disposition (UFD) activities, axially-dependent decay heat source terms were calculated for postirradiation decay up to August 1, 2013 for each assembly in HCNGS casks MPC144 and MPC145. Some of the calculational models and results from this effort serve as the base or reference case for comparison with sensitivity study results obtained using modified methods and models. These comparisons are used to illustrate the degree to which the decay heat source term calculations are sensitive to variations in reactor conditions, analysis methods used, and modeling simplifications made.

Sensitivity study parameters were selected to support examination of the use of potential decay heat calculation simplifications and approximations. For example, modern BWR fuel assemblies include some fuel rods that were fabricated with only $UO_2$ and some rods that were fabricated with a mixture of $UO_2$ and $Gd_2O_3$. One of the sensitivity studies examines the impact on decay heat results of modeling all fuel rods as $UO_2$. This is important because it may not be practical to obtain and model all BWR lattice variations to generate decay heat source terms for use in verifying that clad temperature and clad stress limits are met.

The following sensitivity studies are presented in Section 4.

- Impact of modeling control blade use during reactor operations
- Impact of modeling fuel rods with and without $Gd_2O_3$
- Impact of fuel temperature variation during reactor operations
- Impact of power density variations during reactor operations
- Impact of moderator density variations
- Impact of postirradiation cooling time
- Impact of computational method used to calculate fuel burnup and decay heat
  - Variation in nuclides used to model burned fuel
  - Depletion time step size
  - Dancoff Factors (DFs), resonance self-shielding factors used in multi-group cross-section calculations
  - Use of simplified fuel composition calculations

Each sensitivity study will be discussed in detail in Section 4. The various computational methods used are described in Section 2.2.

## 2.2 Computational Methods and Data

Decay heat calculations involve simulation of fuel burnup in a nuclear reactor and postirradiation cooling time. While the reactor is operating, $^{235}U$ is being consumed through fission reactions, thereby generating fission products. At the same time, some of the uranium is being transmuted to higher actinides (e.g., Np, Pu, Am, Cm, Bk). Some of the actinides may fission, producing fission products, or absorb one or more neutrons or experience radioactive decay, becoming other nuclides. Neutron transport calculations are performed to determine the neutron flux experienced by the fuel. The fluxes are used in fuel composition calculations to determine updated burned-fuel compositions that are then used in the next iteration of flux and fuel composition calculations.

The computer code used in this study is SCALE [3], including release version 6.1 and development version 6.2. SCALE is a code system that includes cross-section processing, depletion, criticality, and shielding computer codes and code sequences. The SCALE codes and code sequences used in the studies presented in this report are further described. Neutron transport calculations were performed using NEWT, a two-dimensional (2D) discrete-ordinates analysis code [3, Section F21]. The ORIGEN-S computer code was used to perform the burned-fuel composition calculations [3, Section F07]. The SCALE computer code system uses sequences to manage running the NEWT and ORIGEN-S computer codes and to handle data communication between them. All calculations performed for this report were conducted using either the TRITON [3, Section T01] or ORIGAMI sequences. ORIGAMI is a new sequence that will be distributed with SCALE 6.2. Additional information on each computer code and sequence is provided in the following subsections.

### 2.2.1 NEWT

The following description of NEWT is taken from the SCALE 6.1 manual, Ref. 3:

> *NEWT (**N**ew **E**SC-based **W**eighting **T**ransport code) is a multigroup discrete-ordinates radiation transport computer code with flexible meshing capabilities that allow two-dimensional (2-D) neutron transport calculations using complex geometric models. The differencing scheme employed by NEWT, the Extended Step Characteristic approach, allows a computational mesh based on arbitrary polygons. Such a mesh can be used to closely approximate curved or irregular surfaces to provide the*

*capability to model problems that were formerly difficult or impractical to model directly with discrete-ordinates methods. Automated grid generation capabilities provide a simplified user input specification in which elementary bodies can be defined and placed within a problem domain. NEWT can be used for eigenvalue, critical-buckling correction, and source calculations, and it can be used to prepare collapsed weighted cross sections in AMPX working library format.*

All NEWT calculations performed for this report used the ENDF/B-VII 238 neutron energy group cross-section data [Section M4.2.4 of Ref. 3] distributed with SCALE 6.1.

NEWT models were created to simulate an infinite 2D array of each fuel assembly axial slice in reactor geometry and conditions. The calculated neutron fluxes were passed to ORIGEN-S to perform zero-dimensional burned-fuel composition calculations.

### 2.2.2 ORIGEN-S

The SCALE ORIGEN-S computer code [3, Section F07] was used to perform all burned-fuel composition calculations. The reference provides the following description:

*ORIGEN (Oak Ridge Isotope Generation code) applies a matrix exponential expansion model to calculate time-dependent concentrations, activities, and radiation source terms for a large number of isotopes simultaneously generated or depleted by neutron transmutation, fission, and radioactive decay. Provisions are made to include continuous nuclide feed rates and continuous chemical removal rates that can be described with rate constants for application to reprocessing or other systems that involve nuclide removal or feed. ORIGEN has been developed and maintained as the depletion and decay module in the SCALE code system. This version, ORIGEN-S, maintains the capability of other versions to be used as a standalone code but has the added ability to utilize multi-energy-group cross sections processed from standard ENDF/B evaluations. Within SCALE, transport codes can be used to model user-defined systems and calculate problem-dependent neutron-spectrum-weighted cross sections that are representative of conditions within any given reactor or fuel assembly, and convert these cross sections into a library that can be used by ORIGEN-S. Time-dependent cross-section libraries may be produced that reflect fuel composition variations during irradiation.*

### 2.2.3 COUPLE

The SCALE COUPLE computer code [3, Section F06] is used with ORIGEN-S to create problem-dependent cross-section libraries that can be used to perform fast fuel depletion calculations. The reactor operating conditions and geometry are implicitly included in the libraries generated by COUPLE. These libraries are used by the ORIGAMI code discussed in Section 2.2.5. The following description of COUPLE is provided in the reference:

*The COUPLE code is used to generate binary format nuclear data libraries that are used by ORIGEN-S to calculate isotopic concentrations and the associated radiation sources and decay heat during irradiation and decay. COUPLE computes weighted, problem-dependent ORIGEN-S neutron cross sections from a multigroup, AMPX working format library. Multigroup infinite dilution AMPX cross-section libraries used by COUPLE are developed from continuous-energy cross-section evaluations of the JEFF-3.0/A neutron activation file. Alternate AMPX libraries based on ENDF/B-V, -VI, or VII cross sections may be applied to an ORIGEN-S library when resonance self-shielding effects are important. The resonance cross-section processing modules and transport codes in the SCALE system may be applied to generate self-shielded cross sections and the weighting spectrum used to collapse cross sections for use by ORIGEN-S. COUPLE combines problem-dependent cross*

*sections with state-of-the-art ENDF/B-VII nuclear decay data and energy-dependent fission product yields to produce libraries that can be used for analyzing a broad range of nuclear applications.*

### 2.2.4 TRITON

TRITON [3, Section T01] is a SCALE sequence that was used for this report to perform fuel burnup and decay heat calculations. TRITON runs the various programs required (e.g., NEWT, KENO-VI, ORIGEN-S and COUPLE), manages the flow of information and data between the programs and generates the output files. Depending upon what the user is trying to accomplish, there are various TRITON sequences that may be used. For this report, the T-DEPL NEWT-based depletion sequence was used. The reference results were generated using the T-DEPL sequence.

### 2.2.5 ORIGAMI

TRITON, through ORIGEN and COUPLE, generates a problem-specific cross-section library that includes all geometric and reactor operating parameter effects. These libraries can be used by ORIGEN to very quickly do additional burnup and decay calculations that are similar to the original NEWT-based depletions. This process has been implemented in a new SCALE sequence called ORIGAMI. The documentation for this new sequence is currently planned to be Section 5.5 in the not-yet-released SCALE 6.2 manual. The fuel depletion calculation methodology is the same as that described for ORIGEN-ARP in Section D01 of the SCALE 6.1 manual [3]. The benefits of this method are that the ORIGAMI calculations are much faster than the original TRITON calculations. An ORIGAMI depletion calculation finishes in about two minutes. A comparable TRITON T-DEPL calculation took three days. Sensitivity studies are presented in Section 4 to compare the resulting decay heat distributions generated by the T-DEPL and ORIGAMI sequences.

The trade-off is that effects of several reactor operating geometry and environment parameters are included in the problem-dependent ORIGEN libraries. Care must be taken by the user to ensure that it is appropriate to use the user-specified problem-dependent library for the system being modeled in ORIGAMI. The following are examples of reactor geometry and environmental conditions that may be implicitly included in the problem-specific libraries:

- Fuel temperature
- Power density
- Presence or absence of control rods
- Presence or absence of other fuel assembly inserts
- Presence or absence of integral burnable absorbers
- Fuel assembly lattice variations (e.g., missing rods, pin pitch variation)
- Soluble boron concentration
- Moderator density (although variation of moderator density can be accounted for in the problem-specific library)
- Fuel density

The effects associated with these factors can be accounted for in depletion calculations by using expanded sets of problem-dependent ORIGEN libraries. For example, sets of libraries may be created at a range of soluble boron concentrations. Then the user would choose the library set with the soluble boron concentration closest to the concentration actually seen in the plant.

A note of caution is in order. Since power density is an ORIGAMI input, one might incorrectly assume that the impact of power density variation on the neutron energy spectrum is properly included. It is not. Instead, the spectral effects are included implicitly in the problem-specific library. ORIGAMI uses the power density with the days of irradiation to calculate burnup. For a small variation in power density, this is not important. However, in a typical BWR assembly, the power density may vary by a factor of 5 to 10 between the peak power density and the power densities seen at the ends of the fuel.

The following description of the ORIGAMI sequence was taken from the draft manual section prepared for SCALE 6.2:

> *ORIGAMI computes detailed isotopic compositions for light water reactor (LWR) assemblies containing $UO_2$ fuel by using the ORIGEN transmutation code with pre-generated ORIGEN libraries, for a specified assembly power distribution. The assembly may be represented by a single lumped model with only an axial power distribution or by a square array of fuel pins with variable pin-powers as well as an axial distribution. In either case, ORIGAMI performs ORIGEN burnup calculations for each of the specified power regions to obtain the spatial distribution of isotopes in the burned fuel. Multiple cycles with varying burn-times and downtimes may be used. ORIGAMI produces several types of output files, including one containing stacked ORIGEN binary output data ("ft71 file") for each depletion zone; files with nuclide concentrations at the last time-step for each axial depletion region, in the format of SCALE standard composition input data or as MCNP material cards; a file containing the axial decay heat at the final time-step; and gamma and neutron radiation source spectra.*

# 3. HOPE CREEK DATA AND REFERENCE RESULTS

In August 2013, temperature measurements were made around spent fuel storage casks stored at the HCNGS site. In support of efforts to perform calculational analysis for comparison with the temperature measurements, staff at Oak Ridge National Laboratory performed detailed decay heat source term calculations.

These calculations were performed with the most detailed data [4] available at the time:

- Assembly average irradiation history for each assembly
- Assembly total initial uranium loading for each assembly
- 25-axial-node initial lattice average enrichment distribution for each assembly
- 25-axial-node irradiation history for each assembly
- 25-axial-node average void fraction for each cycle for each assembly
- Fuel assembly design information for the GE7assemblies (8×8–2 with two small water rods)
- Fuel assembly design information for the GE9 assemblies (8×8–4 with one large water rod)
- Cycle startup and shutdown dates
- 25-axial-node control blade insertion history for the last cycle of each assembly that was next to an inserted control blade in its final cycle of use
- Dates associated with each of the "statepoints" listed in the control blade insertion histories.

Information provided did not include the following:

- Pin-by-pin radially varying initial enrichments
- Axially varying initial uranium loading (i.e., metric tons of uranium per axial zone)
- Number, $Gd_2O_3$ loading per rod, or lattice location of $UO_2$+$Gd_2O_3$ fuel rods
- Control blade dimensions
- Control blade insertion information for cycles other than the last cycle of operation for each assembly
- Fuel temperature data

To support generation of realistic and meaningful sensitivity studies, some of the HCNGS cask decay heat results were used as the reference results for the sensitivity studies presented in Section 4. Table 1 provides the lattice design information for the GE7 and GE9 fuel assemblies used in the sensitivity studies. Figure 1 provides a cross-sectional view of the models for the two assembly designs in the reactor depletion geometry.

Many of the results presented in this report are comparisons with detailed decay heat calculations for HCNGS assembly YJB732, which is a GE9 assembly with an assembly average initial enrichment of 3.23 wt % $^{235}U$, a final discharge burnup of 37.6 GWd/MTU, and a postirradiation decay time of 11.8 years. This assembly was selected for the comparisons because it has one of the highest calculated decay heats of the assemblies stored in HCNGS casks MPC144 and MPC145. Three additional HCNGS assemblies (e.g., LYB665, LYD228 and LYW549) were used for comparisons made in Section 4.7.5, "ORIGAMI." Summary information on each assembly is provided in Section 4.7.5.1.

Since pin-by-pin initial enrichments were not available, the average enrichment was used for all pins in each axial layer (axial enrichment variation was modeled). In the absence of information on the number of, gadolinia content in, and location of $UO_2$+$Gd_2O_3$ fuel pins, the HCNGS fuel was modeled with nine 4 wt % $Gd_2O_3$ fuel pins in each assembly. The locations used for the $Gd_2O_3$ fuel pins are shown in Figure 1, which also shows the control blade model used. The HCNGS reference calculations were performed with the control blades fully inserted for all in-reactor depletion time. Sensitivity study results are provided in Section 4 to show the potential effects of how control blade insertion and $UO_2$+$Gd_2O_3$ fuel rod modeling can affect decay heat generation. The $UO_2$+$Gd_2O_3$ fuel rods are also referred to in this report as gadolinia rods or Gd rods.

The decay heat will vary proportionally to the amount of uranium in each axial zone. Modern BWR fuel assembly designs can include a significant number of part-length fuel rods. Factoring the uranium loading distribution associated with part-length fuel rods into the decay heat results could significantly decrease the decay heat in the top of the assembly and increase the decay heat in the middle and bottom of the assembly. Use of the average uranium loading could result in misprediction of the minimum and maximum fuel rod temperatures in the transportation or storage cask. Consequently, accurate determination of the minimum and maximum decay heat source terms for use in calculating the minimum and maximum fuel rod temperatures requires more detailed information on the initial uranium distribution within each assembly.

The control blade model shown in Figure 1 is "representative" for BWRs and is likely not the design used at HCNGS. This is acceptable because the purpose of including the control blade model is only to demonstrate the potential impacts of control blade presence during fuel composition calculations for decay heat results. In reality, the neutron absorber material, the number of pellet stacks or absorber cylinders, and the dimensions of the blades vary. As is shown in Section 4, the presence of control rods has a small effect initially on decay heat, but the effect increases with decay time. For decay heat purposes, control blade design variation from that used in the studies would produce a small variation in the small increase in decay heat generated due to the presence of control blades.

Detailed initial and cycle average data were provided for each assembly stored in HCNGS casks MPC144 and MPC145. An example of the data is provided in Table 2, in which a negative void fraction means that, in that axial zone, the reactor coolant was cooler than the saturation temperature and the coolant density was higher than the saturation density by that fraction. For each axial zone for each cycle, the moderator density was calculated as the saturated water density (i.e., 0.73917 g/cm$^3$ at 1019.8 psia and 286.13C) multiplied by 1 minus the void faction. The data from Table 2 were used together with the cycle startup and shutdown dates (Ref. 4) provided in Table 3 to set the power density, number of days of irradiation at that power density, the number of shutdown days between cycles, and the postirradiation cooling time. The axially dependent enrichment, power density, and void fraction were modeled for all

assemblies in HGNGS casks MPC144 and MPC145. Some of the results are presented in Section 4 for comparison with the sensitivity cases.

**Table 1. Fuel Assembly Lattice Descriptions**

| Fuel Assembly Lattice Design [a] | GE7 | GE9 |
|---|---|---|
| Fuel Rods | | |
| Pellet Outer Diameter (cm) | 1.0566 | 1.0439 |
| Clad Inner Diameter (cm) | 1.0795 | 1.0643 |
| Clad Outer Diameter (cm) | 1.2268 | 1.2268 |
| Clad Material (cm) | zircaloy-2[b] | zircaloy-2 |
| Pin Pitch (cm) | 1.6256 | 1.6256 |
| Lattice | 8×8–2 | 8×8–4 |
| Water Rods | | |
| Number | 2 | 1 |
| Fuel Rods Displaced | 2 | 4 |
| Inner Diameter (cm) | 1.3487 | 3.2004 |
| Outer Diameter (cm) | 1.5011 | 3.4036 |
| Material | zircaloy-2 | zircaloy-2 |
| $UO_2$+$Gd_2O_3$ Rods | | |
| Number | 9 | 9 |
| $Gd_2O_3$ (wt %) | 4 | 4 |
| Fuel Assembly Channel | | |
| Inner Dimension (cm) | 13.4061 | 13.4061 |
| Wall Thickness (cm) | 0.2032 | 0.2032 |
| Material | zircaloy-2 | zircaloy-2 |

[a] Dimensions from Reference 4.
[b] References describe the material only as zircaloy.

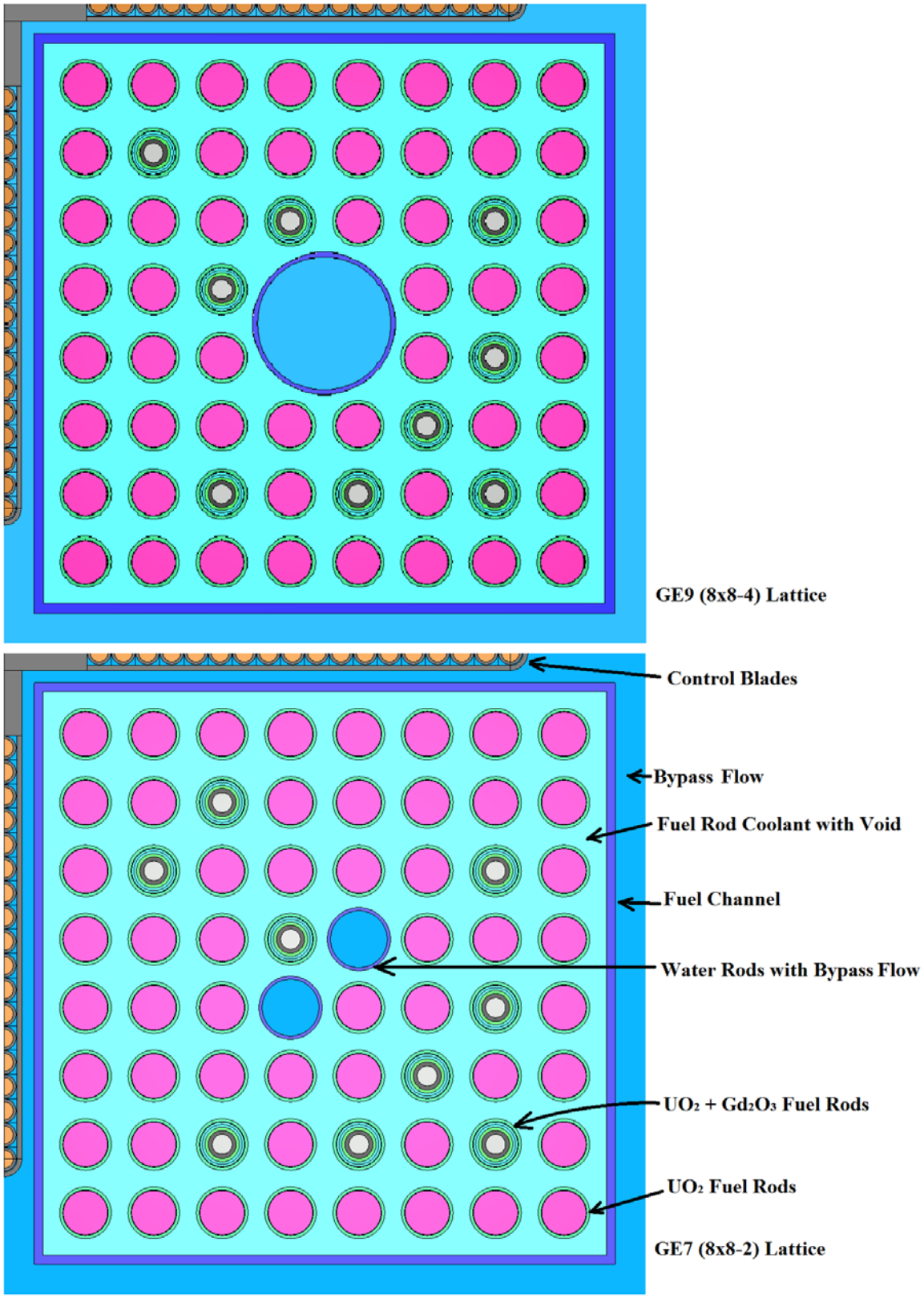


**Figure 1. GE9 (top) and GE7 (bottom) lattices used in the sensitivity studie**

**Table 2. HCNGS Fuel Assembly Irradiation History Data File for Assembly YJB732**

| Axial Zone[a] | Lattice ID | Initial Enrich.[b] | Cycle | Burnup[c] | Void Fraction | Cycle | Burnup | Void Fraction | Cycle | Burnup | Void Fraction | Cycle | Burnup | Void Fraction |
|---|---|---|---|---|---|---|---|---|---|---|---|---|---|---|
| YJB732[d] 178424.04 | | | | | | | | | | | | | | |
| 25 | 23 | 0.71 | 7 | 2998.07 | 0.8293 | 8 | 5283.12 | 0.8051 | 9 | 6343.21 | 0.7637 | 10 | 7148.92 | 0.7341 |
| 24 | 11 | 0.71 | 7 | 4606.41 | 0.8305 | 8 | 8236.08 | 0.8053 | 9 | 10051.30 | 0.7602 | 10 | 11483.50 | 0.7276 |
| 23 | 22 | 3.5 | 7 | 11844.30 | 0.8296 | 8 | 20217.40 | 0.8053 | 9 | 24540.30 | 0.7599 | 10 | 27912.20 | 0.7274 |
| 22 | 22 | 3.5 | 7 | 14917.80 | 0.8246 | 8 | 25045.30 | 0.7999 | 9 | 30320.00 | 0.7538 | 10 | 34232.20 | 0.7220 |
| 21 | 22 | 3.5 | 7 | 17104.60 | 0.8173 | 8 | 28353.60 | 0.7922 | 9 | 34227.90 | 0.7453 | 10 | 38408.10 | 0.7139 |
| 20 | 13 | 3.66 | 7 | 18569.70 | 0.8078 | 8 | 30759.30 | 0.7819 | 9 | 37121.10 | 0.7336 | 10 | 41490.00 | 0.7021 |
| 19 | 13 | 3.66 | 7 | 19424.20 | 0.7963 | 8 | 32165.90 | 0.7695 | 9 | 38806.80 | 0.7196 | 10 | 43180.00 | 0.6883 |
| 18 | 13 | 3.66 | 7 | 19831.00 | 0.7828 | 8 | 32911.10 | 0.755 | 9 | 39721.50 | 0.7032 | 10 | 44061.90 | 0.6718 |
| 17 | 13 | 3.66 | 7 | 19918.70 | 0.7677 | 8 | 33241.40 | 0.7386 | 9 | 40136.10 | 0.6848 | 10 | 44501.00 | 0.6525 |
| 16 | 13 | 3.66 | 7 | 20099.00 | 0.7506 | 8 | 33718.40 | 0.7201 | 9 | 40708.70 | 0.6642 | 10 | 45047.80 | 0.6315 |
| 15 | 13 | 3.66 | 7 | 20203.90 | 0.7313 | 8 | 34020.60 | 0.6989 | 9 | 41041.10 | 0.6411 | 10 | 45332.60 | 0.6080 |
| 14 | 13 | 3.66 | 7 | 20243.80 | 0.7096 | 8 | 34150.80 | 0.6751 | 9 | 41141.00 | 0.6156 | 10 | 45439.90 | 0.5814 |
| 13 | 13 | 3.66 | 7 | 20498.70 | 0.6849 | 8 | 34542.50 | 0.6482 | 9 | 41539.30 | 0.5872 | 10 | 45774.00 | 0.5527 |
| 12 | 13 | 3.66 | 7 | 20652.40 | 0.6563 | 8 | 34719.60 | 0.617 | 9 | 41691.30 | 0.5546 | 10 | 45822.60 | 0.5203 |
| 11 | 13 | 3.66 | 7 | 20707.30 | 0.6226 | 8 | 34689.50 | 0.5806 | 9 | 41608.20 | 0.5173 | 10 | 45692.00 | 0.4829 |
| 10 | 12 | 3.5 | 7 | 20054.90 | 0.5842 | 8 | 33565.50 | 0.5392 | 9 | 40276.00 | 0.4751 | 10 | 44223.10 | 0.4408 |
| 9 | 12 | 3.5 | 7 | 20202.70 | 0.5405 | 8 | 33606.50 | 0.4925 | 9 | 40278.20 | 0.4289 | 10 | 44075.60 | 0.3967 |
| 8 | 12 | 3.5 | 7 | 20333.50 | 0.4885 | 8 | 33596.30 | 0.4379 | 9 | 40163.10 | 0.3768 | 10 | 43758.10 | 0.3482 |
| 7 | 12 | 3.5 | 7 | 20420.60 | 0.4264 | 8 | 33466.80 | 0.3744 | 9 | 39828.20 | 0.3188 | 10 | 43268.70 | 0.2940 |
| 6 | 12 | 3.5 | 7 | 20783.70 | 0.351 | 8 | 33649.40 | 0.2999 | 9 | 39764.90 | 0.2543 | 10 | 42974.90 | 0.2347 |
| 5 | 12 | 3.5 | 7 | 20924.50 | 0.2581 | 8 | 33424.80 | 0.2114 | 9 | 39205.00 | 0.1785 | 10 | 42168.90 | 0.1649 |
| 4 | 12 | 3.5 | 7 | 20508.10 | 0.1451 | 8 | 32359.40 | 0.1104 | 9 | 37701.30 | 0.0925 | 10 | 40479.30 | 0.0850 |
| 3 | 12 | 3.5 | 7 | 18945.50 | 0.0332 | 8 | 29760.80 | 0.0183 | 9 | 34617.30 | 0.0132 | 10 | 37173.80 | 0.0109 |
| 2 | 12 | 3.5 | 7 | 14132.80 | -0.0202 | 8 | 22761.30 | -0.0201 | 9 | 26784.50 | -0.0202 | 10 | 28982.10 | -0.0203 |
| 1 | 11 | 0.71 | 7 | 3024.34 | -0.0217 | 8 | 5068.06 | -0.0215 | 9 | 6083.64 | -0.0215 | 10 | 6653.78 | -0.0216 |

[a] Axial zone number, zone 1 is the bottom of the active fuel length.
[b] Axial zone average initial enrichment in wt % $^{235}U$.
[c] Assembly axial zone accumulated burnup in MWd/MTU.
[d] Assembly ID, initial uranium mass in grams, and number of cycles the assembly was used.

**Table 3. HCNGS Startup and Shutdown Data**

| Cycle | Startup Date | Shutdown Date | Number Days Up | Number Days Down | Days Since Shutdown Through 8/1/2013 |
|---|---|---|---|---|---|
| 1 | 6/28/1986 | 2/13/1988 | 595 | 57 | 9301 |
| 2 | 4/10/1988 | 9/16/1989 | 524 | 61 | 8720 |
| 3 | 11/16/1989 | 12/25/1990 | 404 | 53 | 8255 |
| 4 | 2/16/1991 | 9/12/1992 | 574 | 55 | 7628 |
| 5 | 11/6/1992 | 3/5/1994 | 484 | 51 | 7089 |
| 6 | 4/25/1994 | 11/11/1995 | 565 | 128 | 6473 |
| 7 | 3/18/1996 | 9/10/1997 | 541 | 81 | 5804 |
| 8 | 11/30/1997 | 2/13/1999 | 440 | 45 | 5283 |
| 9 | 3/30/1999 | 4/22/2000 | 389 | 30 | 4849 |
| 10 | 5/22/2000 | 10/11/2001 | 507 | 21 | 4312 |
| 11 | 11/1/2001 | 4/16/2003 | 531 | 26 | 3760 |
| 12 | 5/12/2003 | 10/10/2004 | 517 | - | 3217 |

# 4. DECAY HEAT SENSITIVITY STUDIES

A series of sensitivity studies were performed to evaluate the potential impact of various approximations and simplifications and to evaluate the adequacy of various calculational techniques. Validation of decay heat calculations is beyond the scope of the work presented herein. However, validation of UNF composition and decay heat calculations have been the subject of many studies, including References 5, 6, 7, 8, 9, and 10, among others.

Each subsection of Section 4 covers a separate sensitivity study and includes a description of the variations, the nature of the sensitivity calculations performed, the study results, and some observations and conclusions.

In general, the parameters examined in the sensitivity studies were evaluated as though they were all independent of each other. This is not realistic. For example, moderator density tends to decrease as power density increases. This becomes particularly important if the parameters are anticorrelated such as in the case of control blade usage and moderator density. The use of control blades causes decay heat to be higher; but typically also results in higher moderator densities, which causes decay heat to be lower. Users of the data in this report may need to consider correlations between parameters.

## 4.1 Control Blade Use Modeling

The original HCNGS decay heat calculations assumed that modeling with control blades fully inserted for all cycles would yield conservatively high decay heat values. In this subsection the reference results are compared with results when other control blade use strategies are modeled. In particular, the calculations for axial zone 15 in assembly YJB732, which was used in the HCNGS for four cycles, accumulating a zone average burnup of 45.33 GWd/MTU and had a postirradiation cooling time of 11.8 years, were run again with various cycle-long control blade insertions modeled. Table 4 presents the configurations

modeled, the decay heat results, and the percentage difference from reference value (i.e., control blade used in cycles 7 through 10), which are sorted from top to bottom with increasing decay heat.

**Table 4. Sensitivity of Decay Heat to Control Blade Usage**

| Control Blade Use (1 = in & 0 = out) | | | | Decay Heat on 8/1/2013 | Difference from reference value |
|---|---|---|---|---|---|
| Cy 7 | Cy 8 | Cy 9 | Cy 10 | (Watts/MTU) | (%) |
| 0 | 0 | 0 | 0 | 1.464E+03 | -3.3 |
| 1 | 0 | 0 | 0 | 1.466E+03 | -3.2 |
| 0 | 1 | 0 | 0 | 1.477E+03 | -2.5 |
| 1 | 1 | 0 | 0 | 1.480E+03 | -2.3 |
| 0 | 0 | 1 | 0 | 1.483E+03 | -2.1 |
| 0 | 0 | 0 | 1 | 1.484E+03 | -2.0 |
| 1 | 0 | 1 | 0 | 1.485E+03 | -2.0 |
| 1 | 0 | 0 | 1 | 1.485E+03 | -2.0 |
| 0 | 1 | 1 | 0 | 1.496E+03 | -1.2 |
| 0 | 1 | 0 | 1 | 1.496E+03 | -1.2 |
| 1 | 1 | 0 | 1 | 1.497E+03 | -1.1 |
| 1 | 1 | 1 | 0 | 1.497E+03 | -1.1 |
| 0 | 0 | 1 | 1 | 1.502E+03 | -0.8 |
| 1 | 0 | 1 | 1 | 1.503E+03 | -0.8 |
| 0 | 1 | 1 | 1 | 1.513E+03 | -0.1 |
| 1 | 1 | 1 | 1 | **1.514E+03**[a] | **0** |

[a] Reference value.

The results show that modeling of control blades does increase decay heat. Actual operations are likely closer to one cycle of operation with a control blade inserted next to the assembly. The full swing between all rodded and all unrodded data provides only a 3.4 % change in decay heat. Depending on the nature of the safety analysis being performed, decay heat may be minimized by modeling no control blade insertion and may be maximized by modeling full insertion for all cycles. It has been suggested that it may be appropriate to model control blade insertion in only the last cycle of an assembly's use. This may be acceptable if being a couple of percent too high or too low is acceptable.

Additional decay heat calculations were performed using the assembly YJB732 axial zone 15 to explore the variation in the effects of control blades as a function of burnup and cooling time. Table 5 shows the change in decay heat between depletion without and with control blades present. In general, the presence of control blades during depletion results in increasingly higher decay heat at higher burnups and higher cooling times.

**Table 5. Decay Heat Variation Due to Control Blade Modeling Variation**

| | Postirradiation Cooling Times (years) | | | | | | | | |
|---|---|---|---|---|---|---|---|---|---|
| Burnup | 0 | 5 | 10 | 11.8 | 20 | 40 | 60 | 80 | 100 |
| (GWd/MTU) | Decay Heat (Watts / MTU) for Cases Depleted Without Control Blades | | | | | | | | |
| 20.2 | 2.32E+06 | 1.03E+03 | 6.51E+02 | 6.14E+02 | 5.15E+02 | 3.65E+02 | 2.69E+02 | 2.06E+02 | 1.65E+02 |
| 34.0 | 1.92E+06 | 1.77E+03 | 1.15E+03 | 1.08E+03 | 8.99E+02 | 6.40E+02 | 4.75E+02 | 3.68E+02 | 2.97E+02 |
| 41.0 | 1.10E+06 | 2.06E+03 | 1.41E+03 | 1.33E+03 | 1.10E+03 | 7.79E+02 | 5.76E+02 | 4.45E+02 | 3.59E+02 |
| 45.3 | 5.20E+05 | 2.11E+03 | 1.55E+03 | 1.46E+03 | 1.22E+03 | 8.59E+02 | 6.34E+02 | 4.89E+02 | 3.94E+02 |
| | Decay Heat (Watts / MTU) for Cases Depleted With Control Blades | | | | | | | | |
| 20.2 | 2.31E+06 | 1.05E+03 | 6.58E+02 | 6.21E+02 | 5.25E+02 | 3.81E+02 | 2.88E+02 | 2.26E+02 | 1.86E+02 |
| 34.0 | 1.92E+06 | 1.82E+03 | 1.18E+03 | 1.11E+03 | 9.32E+02 | 6.82E+02 | 5.21E+02 | 4.15E+02 | 3.44E+02 |
| 41.0 | 1.10E+06 | 2.11E+03 | 1.45E+03 | 1.37E+03 | 1.15E+03 | 8.38E+02 | 6.40E+02 | 5.09E+02 | 4.22E+02 |
| 45.3 | 5.19E+05 | 2.16E+03 | 1.60E+03 | 1.51E+03 | 1.28E+03 | 9.30E+02 | 7.09E+02 | 5.65E+02 | 4.68E+02 |
| | % Change in Decay Heat from Depletion With Control Blades to Depletion Without Control Blades | | | | | | | | |
| 20.2 | 0.2 | -2.0 | -1.1 | -1.2 | -1.8 | -4.1 | -6.5 | -8.8 | -10.9 |
| 34.0 | 0.2 | -2.7 | -2.5 | -2.6 | -3.5 | -6.2 | -8.8 | -11.3 | -13.5 |
| 41.0 | 0.2 | -2.7 | -2.9 | -3.1 | -4.1 | -7.0 | -9.9 | -12.6 | -14.9 |
| 45.3 | 0.3 | -2.6 | -3.1 | -3.3 | -4.5 | -7.6 | -10.6 | -13.4 | -15.8 |

## 4.2 Gadolinia Fuel Rod Modeling

Fuel assemblies used in BWRs typically include some fuel rods that are fabricated with a mixture of $UO_2$ and $Gd_2O_3$. They are sometimes referred to as “gadolinium bearing fuel rods,” “gadolinia rods,” “gad rods,” or “gad fuel rods.” The number of gadolinia rods used in an assembly varies as the core reload designer varies the design to meet energy requirements and safety limits. Gadolinia rod data are not available for the HCNGS fuel, but are available for three other BWRs that have utilized GE 8×8 lattices.

The Quad Cities Unit 2 reactor used GE7, 8, 9 and 10 fuel assemblies in cycles 9 through 14 [11]. The assembly designs are 8×8 lattices. All enriched fuel assemblies documented in the reference used between 7 and 10 gadolinia rods. The gadolinia rods were loaded with either 3 or 4 wt % $Gd_2O_3$.

The LaSalle Unit 1 reactor used GE9B fuel as fresh assemblies in cycles 4 through 8 [12]. This assembly design is an 8×8 lattice. All enriched fuel assemblies documented in the reference used between 7 and 12 gadolinia rods. The gadolinia rods were loaded with either 3, 4, or 5 wt % $Gd_2O_3$.

The Grand Gulf Unit 1 reactor used ENC8×8, ANF8×8, LTA9×9–5, ANF9×9–5 and SNP9×9–5 fuel as feed assemblies in cycles 2 through 8 [13]. These assembly designs are 8x8 and 9x9 lattices. All enriched fuel assemblies documented in the reference used between 5 and 10 gadolinia rods. The gadolinia rods were loaded with between 3 and 7 wt % $Gd_2O_3$.

The HCNGS decay heat calculations used nine gadolinia rods loaded with 4 wt % $Gd_2O_3$. These values were considered adequately representative compared to information available for real BWR fuel bundles.

A sensitivity study was performed with the gadolinia rods replaced with unpoisoned $UO_2$ rods. The total decay heat for assembly YJB732 burned to 37.6 GWd/MTU and cooled for 11.8 years was 0.2146 kW with the gadolinia rods modeled and 0.2144 kW without the gadolinia rods. Thus the modeling of the

gadolinia rods made an insignificant difference in the resulting decay heat. This result is not entirely unexpected. The gadolinium nuclides built into the assembly are effectively used up by the end of the first cycle of operation. As can be seen for control blade use in Table 4, there was no difference in decay heat between having the control blades fully inserted for the entire first cycle and having no control blades in any cycle. Thus the gadolinia rod results are consistent with the control blade use results.

The model used for axial zone 15 of HCNGS assembly YJB732 was used to recalculate the decay heat for that axial zone at various burnups and postirradiation cooling times. Not modeling $Gd_2O_3$ rods may cause a small underestimation of decay heat at longer decay times.

**Table 6. Decay Heat Variation Due to $Gd_2O_3$ Rod Modeling Variation**

| | Postirradiation Cooling Times (years) | | | | | | | | |
|---|---|---|---|---|---|---|---|---|---|
| Burnup | 0 | 5 | 10 | 11.8 | 20 | 40 | 60 | 80 | 100 |
| (GWd/MTU) | Decay Heat (Watts / MTU) for Cases Depleted Without $Gd_2O_3$ Rods | | | | | | | | |
| 20.2 | 2.32E+06 | 1.05E+03 | 6.59E+02 | 6.21E+02 | 5.23E+02 | 3.76E+02 | 2.82E+02 | 2.20E+02 | 1.79E+02 |
| 34.0 | 1.92E+06 | 1.82E+03 | 1.18E+03 | 1.11E+03 | 9.29E+02 | 6.76E+02 | 5.15E+02 | 4.08E+02 | 3.37E+02 |
| 41.0 | 1.10E+06 | 2.12E+03 | 1.45E+03 | 1.37E+03 | 1.15E+03 | 8.33E+02 | 6.33E+02 | 5.02E+02 | 4.15E+02 |
| 45.3 | 5.19E+05 | 2.16E+03 | 1.59E+03 | 1.51E+03 | 1.28E+03 | 9.24E+02 | 7.03E+02 | 5.58E+02 | 4.61E+02 |
| | Decay Heat (Watts / MTU) for Cases Depleted With $Gd_2O_3$ Rods | | | | | | | | |
| 20.2 | 2.31E+06 | 1.05E+03 | 6.58E+02 | 6.21E+02 | 5.25E+02 | 3.81E+02 | 2.88E+02 | 2.26E+02 | 1.86E+02 |
| 34.0 | 1.92E+06 | 1.82E+03 | 1.18E+03 | 1.11E+03 | 9.32E+02 | 6.82E+02 | 5.21E+02 | 4.15E+02 | 3.44E+02 |
| 41.0 | 1.10E+06 | 2.11E+03 | 1.45E+03 | 1.37E+03 | 1.15E+03 | 8.38E+02 | 6.40E+02 | 5.09E+02 | 4.22E+02 |
| 45.3 | 5.19E+05 | 2.16E+03 | 1.60E+03 | 1.51E+03 | 1.28E+03 | 9.30E+02 | 7.09E+02 | 5.65E+02 | 4.68E+02 |
| | % Change in Decay Heat from Depletion Without $Gd_2O_3$ Rods to Depletion With $Gd_2O_3$ Rods | | | | | | | | |
| 20.2 | -0.3 | 0.1 | 0.0 | 0.0 | 0.4 | 1.2 | 2.1 | 3.0 | 3.8 |
| 34.0 | -0.1 | -0.1 | 0.1 | 0.1 | 0.3 | 0.8 | 1.3 | 1.7 | 2.1 |
| 41.0 | 0.0 | -0.2 | 0.1 | 0.2 | 0.3 | 0.7 | 1.0 | 1.4 | 1.6 |
| 45.3 | 0.0 | -0.1 | 0.1 | 0.2 | 0.3 | 0.6 | 0.9 | 1.2 | 1.5 |

## 4.3 Fuel Temperature Modeling

The fuel temperature during power operations affects the decay heat through temperature-related Doppler broadening of resonance absorption cross sections. Increased temperatures cause the absorption resonances to broaden, thereby increasing the probability that a neutron will be absorbed into non-fissile nuclides. Thus $^{238}U$ becomes $^{239}U$, which decays to $^{239}Np$, which in turn decays to $^{239}Pu$. These nuclides also have an increased chance to absorb another neutron, thereby transmuting to even heavier actinides. Higher fuel temperatures are expected to result in higher decay heat at longer decay times because the dominating nuclides for decay heat at long decay times (e.g., 100-year decay time) are $^{241}Am$ and $^{238}Pu$ (NUREG-CR/6700, Ref. 14).

Fuel temperature data were not available for the HCNGS decay heat calculations. Consequently, a fuel temperature of 1000K (727ºC) was assumed for the HCNGS calculations. A review of references 11, 12, and 13 showed that the fuel temperatures used for modeling these reactor configurations ranged up to nearly 1400K. Figure 2 shows a plot of fuel temperatures in the peak temperature node for six assemblies from three different reactors. In the plot, “LS1” stands for LaSalle Unit 1, “QC2” stands for Quad Cities Unit 2, and “GG” stands for Grand Gulf. Specific assembly identifiers and node numbers are also provided. The plot shows that for these examples, a fuel temperature of 1000K is reasonably

representative. As one should expect, the higher temperatures generally occur earlier in an assembly's life when the assembly is most reactive. Significant temperature swings are due to insertion and removal of control blades for reactivity and power distribution control. Figure 3 shows the axial temperature profile for LaSalle Unit 1 assembly D16 at its peak fuel temperature.

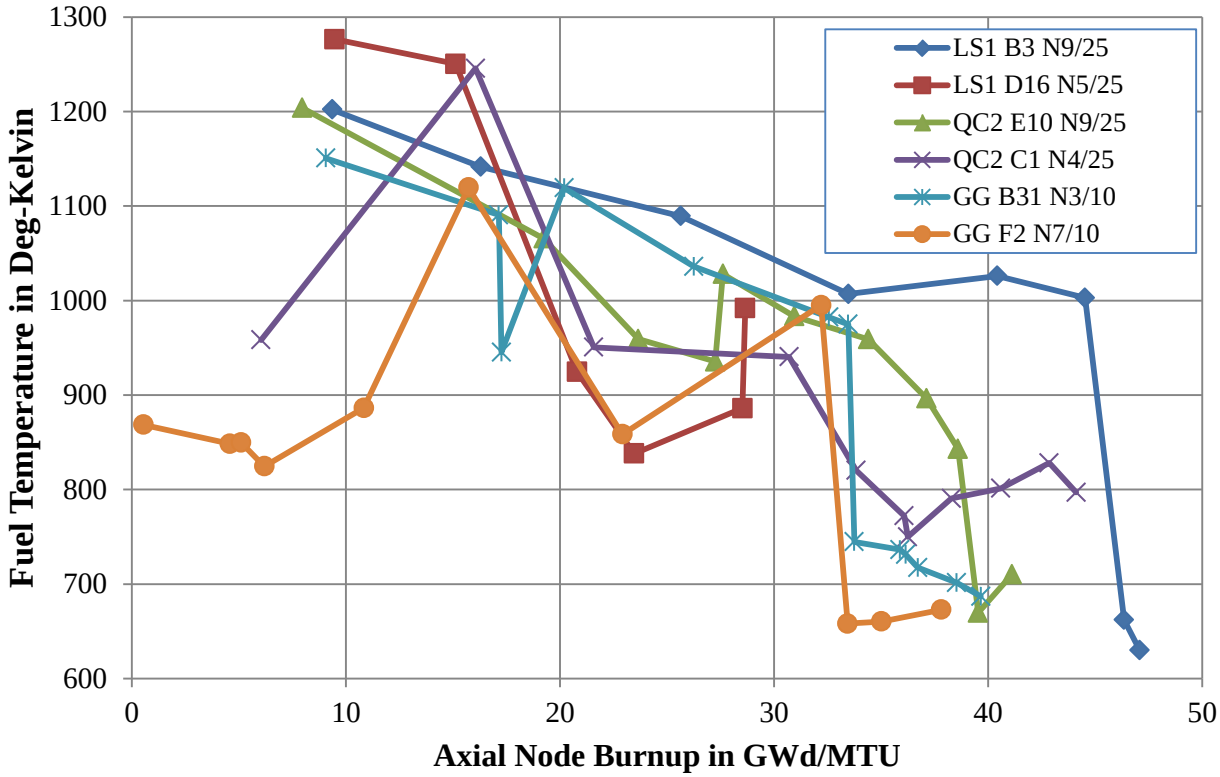


**Figure 2. Fuel temperatures used in modeling six assemblies in three critical reactor models**

To explore the impact of fuel temperature on decay heat, the decay heat for assembly YJB732 was recalculated using 800K, 900K and 1100K fuel temperatures. Table 7 provides the results of the sensitivity studies. The variation in the decay heat due to fuel temperature is small (i.e., a few tenths of a percent).

**Table 7. Decay Heat Variation with Fuel Temperature for Assembly YJB732**

| Fuel Temperature (degrees K) | Decay Heat [a] (kW) | Difference from 1000K Value (%) |
|---|---|---|
| 800 | 0.2142 | -0.2 |
| 900 | 0.2144 | -0.1 |
| 1000 | 0.2146 | Reference value |
| 1100 | 0.2148 | 0.1 |

[a] 11.8-year decay time.

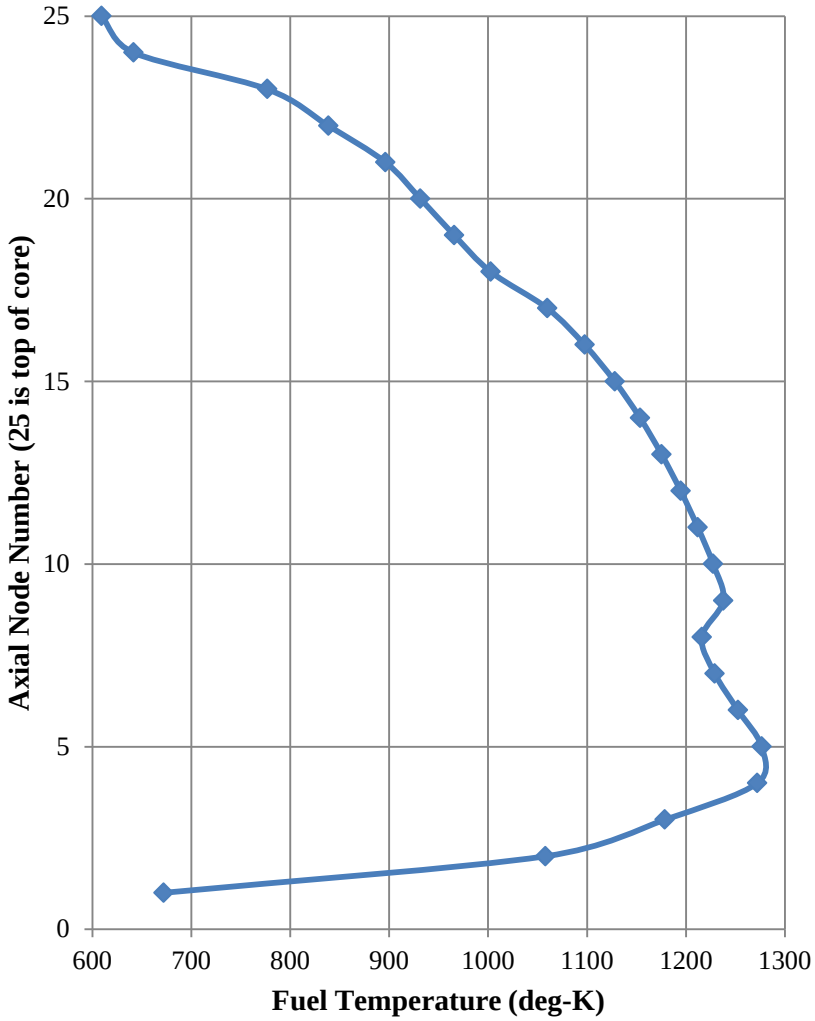


**Figure 3. Axial fuel temperature distribution for LaSalle Unit 1 assembly D16 at peak fuel temperature (from datapoint 6 in Table 4-69 of Ref. 12)**

The decay heat results in Table 7 indicate that the decay heat following significant decay periods (i.e., years) is only slightly sensitive to the fuel temperature used in the decay heat calculations.

## 4.4 Power Density Modeling

Due to the use of control blades to control reactivity and power distribution in BWR cores, the axially varying power density experienced by an assembly may vary considerably over its life. This leaves the analyst with the option of either finding and modeling the detailed time-dependent and axially dependent power density or adopting a conservative value for use in decay heat calculations.

To support selection of a conservative power density, sensitivity studies were performed to show how the power density affects decay heat. A GE7 fuel assembly was modeled with two gadolinia rods and a uranium enrichment of 5 wt % $^{235}$U. The number of days of depletion was modified such that the product of the power density and days of irradiation was equal to 70 GWd/MTU. The calculations were performed for 5, 20, and 50 years of postirradiation cooling time. Table 8 presents the results and includes a column showing the percentage change from the 25 MW/MTU case, which was selected as the

reference case because it is close to typical core-average power densities in modern BWRs. Higher power densities result in higher decay heat; the shorter cooling time cases are much more sensitive to the power density variation than are longer cooling time cases.

**Table 8. Variation of Decay Heat with Power Density and Decay Time**

| Power Density (MW/MTU) | Decay Heat | | | | | |
|---|---|---|---|---|---|---|
| | 5 years [a] | | 20 years [a] | | 50 years [a] | |
| | kW/MTU | % diff | kW/MTU | % diff | kW/MTU | % diff |
| 10 | 3.05 | -17.5 | 1.83 | -5.5 | 1.07 | -2.5 |
| 15 | 3.34 | -9.8 | 1.89 | -2.5 | 1.08 | -1.1 |
| 20 | 3.55 | -4.2 | 1.92 | -0.9 | 1.09 | -0.3 |
| **25** | **3.70** | **Reference** | **1.94** | **Reference** | **1.09** | **Reference** |
| 30 | 3.83 | 3.6 | 1.95 | 0.7 | 1.10 | 0.3 |
| 35 | 3.94 | 6.6 | 1.96 | 1.1 | 1.10 | 0.5 |
| 40 | 4.04 | 9.1 | 1.97 | 1.5 | 1.10 | 0.6 |

[a] Decay time.

The sensitivity decreases significantly for longer postirradiation cooling times, as shown graphically in Figure 4.

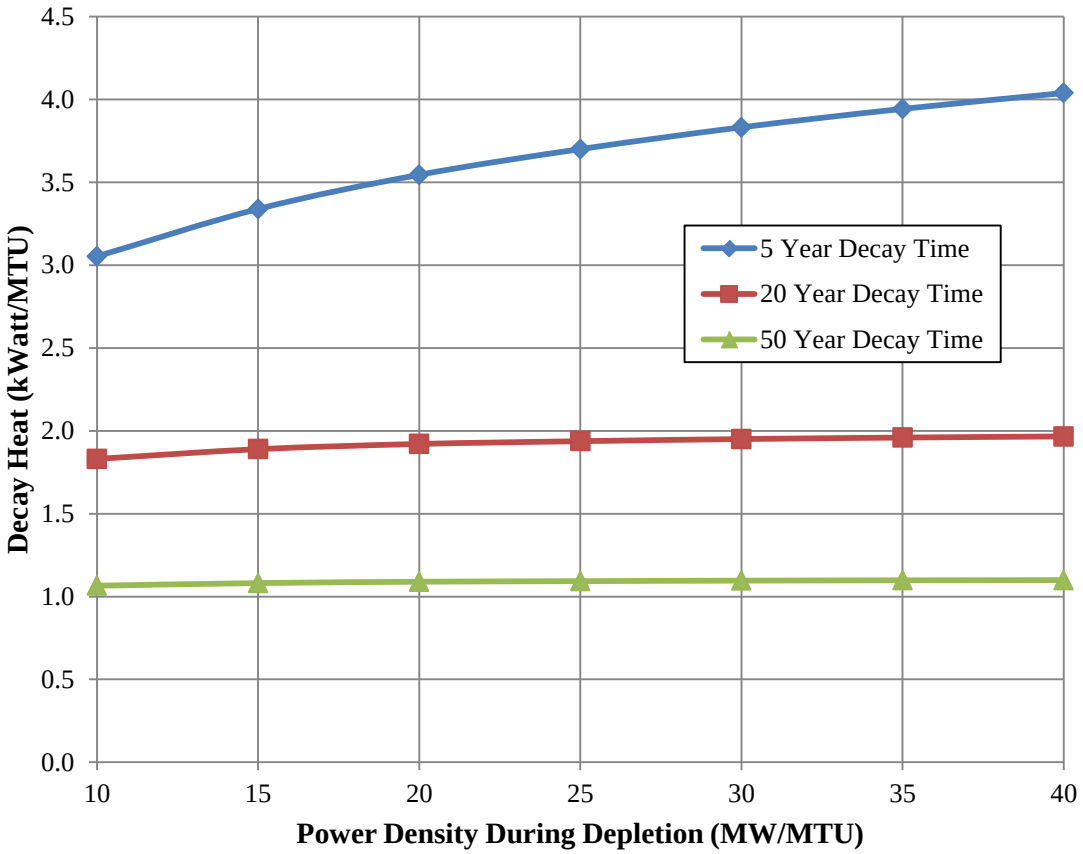


**Figure 4. Sensitivity of decay heat to power density used in fuel depletion calculations**

Another question one might ask is whether it is acceptable to model average power density experienced by an assembly rather than the time- or cycle-dependent power density. The decay heat for HCNGS assembly YJB732 was recalculated using the axially dependent burnup-averaged power density. The average power density was calculated as the axial zone final burnup divided by the number of days of at-power operation. The decay heat for the average-power-density case increased 1.9% to 0.2187 kW from the 0.2146 kW reference value from the detailed calculation. In general, use of the life-time-average power density shifts burnup from the early cycles to later in assembly life.

## 4.5 Enrichment and Moderator Density Variation

In a BWR, the effective density (i.e., including the effect of voids) of the moderator cooling the fuel pins can vary from around 0.75 g/cm$^3$ in the bottom of the core to 0.15 g/cm$^3$ in the top. The density can also change significantly in the areas where control blades are inserted or withdrawn.

For comparison with the detailed results for assembly YJB732, in which the moderator density is modeled on a cycle-average and axially varying basis, two additional calculation variations were generated. In the first case, the moderator density was modeled as the burnup-averaged moderator density averaged over the assembly life. For that case, the axial moderator density variation was simulated. In the second case, a single average moderator density was used for all axial zones and all cycles. Table 9 provides the results from the sensitivity study. The study indicates that it may be appropriate to use the moderator density averaged over the life of the assembly and averaged over the axial distribution.

**Table 9. Variation in Assembly YJB732 Calculated Decay Heat due to Modeling Simplifications**

| Case | Moderator Density | | Assembly Decay Heat (kW) | Diff. from Reference (%) |
|---|---|---|---|---|
| | Cycle Variation | Axial Variation | | |
| Reference | Cycle Avg. | Distributed | 0.21463 | 0 |
| Axially Varying | Life Avg. | Distributed | 0.21581 | 0.5 |
| Assembly Average | Life Avg. | Axial Avg. | 0.21487 | 0.1 |

A more generic study was performed to provide additional insight concerning the impact of variation in moderator density on calculated decay heat. In that study the depletion history of assembly YJB732 was used with the assembly life-time average power density (i.e., 20.0 MW/MTU), variable moderator densities (i.e., 0.1 to 0.8 g/cm$^3$), and variable postirradiation decay times (i.e. 5 to 100 years). The calculations were performed using the SCALE ORIGAMI sequence (see Section 2.2.5) and the UFD nominal GE8×8 depletion library (i.e., G4608G4B). The decay heat results presented in Figure 5 are in kilowatts per metric tons of uranium.

For the same burnup, decay heat increases with lower enrichment, lower moderator density, and shorter postirradiation cooling times. The effects on decay heat associated with enrichment and cooling density are smaller at longer cooling times.

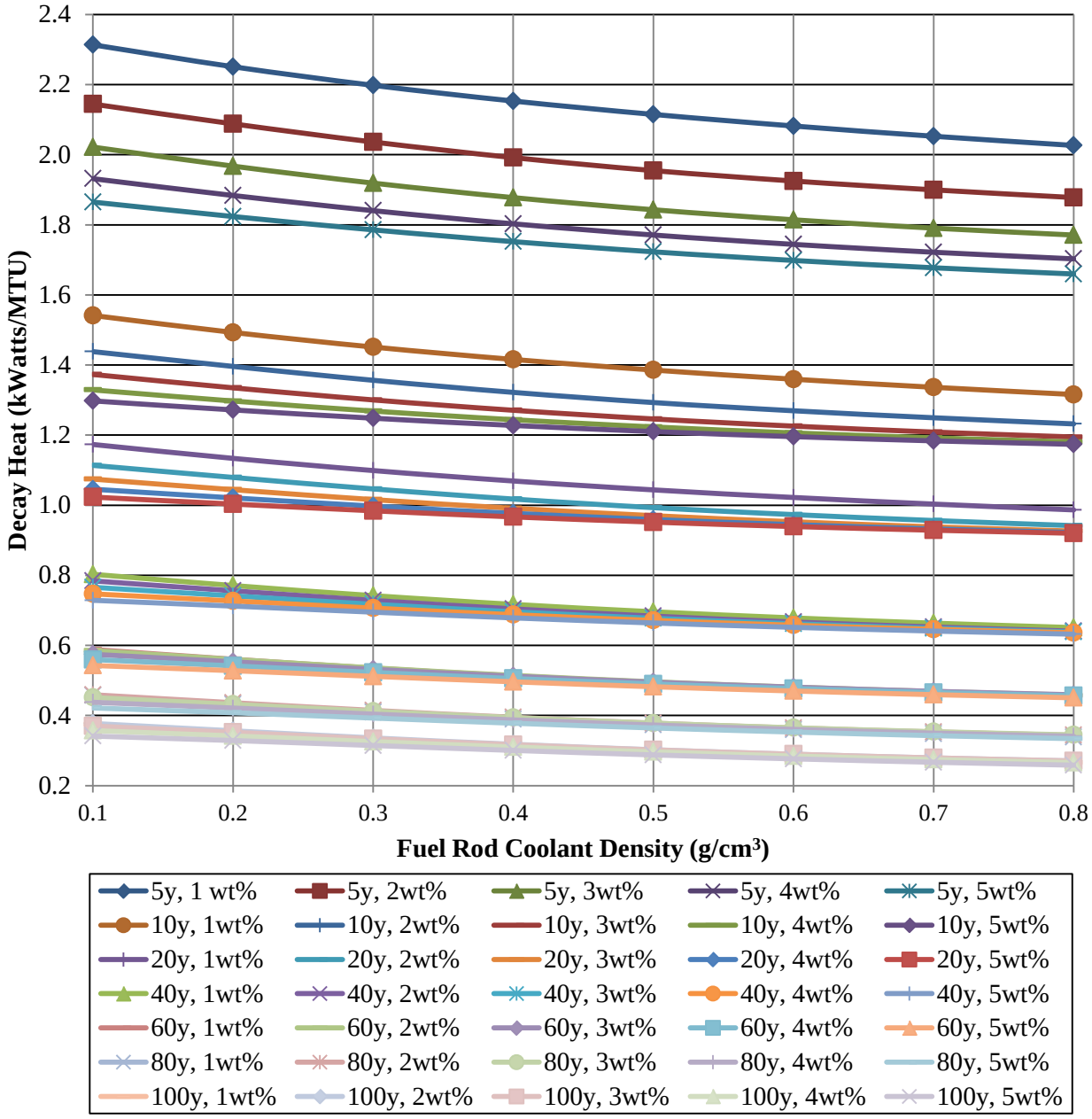


**Figure 5. Decay heat in kilowatts per metric tons of uranium as a function of fuel rod coolant density, fuel initial enrichment and postirradiation cooling time**

## 4.6 Postirradiation Cooling Time

Decay heat is produced by radioactive decay of unstable nuclides. Consequently, as the radioactive nuclides decay to eventually become stable nuclides, fewer and fewer radioactive nuclides remain to decay in the future. Following reactor shutdown, most of the decay heat comes from the decay of short half-life nuclides. As the short-half-life inventory reduces with time, the primary decay heat producers become the heavier actinides. While the behavior of decay heat as a function of time after shutdown is

well known, less well understood is how assembly design variations and reactor conditions affect the postirradiation cooling time behavior of decay heat.

In general terms, anything that causes the neutron energy spectrum to shift toward higher energies increases plutonium production. Many of the higher actinides, including plutonium, have half-lives greater than 10 years. Thus the accurate modeling of the in-growth of the higher actinides is important for storage and transport casks decay heat analysis. Trends of decay heat variation with some of the primary in-reactor factors influencing in-growth of higher actinides were presented earlier in this report.

One factor that could be overlooked is the variation of decay heat with initial enrichment. The physics involved is that for a lower enrichment fuel to achieve the same burnup as fuel having a higher initial enrichment, more of the fission must come from the in-growth and fission of plutonium. Table 10 and Figure 6 show the behavior of decay heat as a function of initial average enrichment and postirradiation cooling time. The assembly lifetime average moderator density (i.e., 0.3414 g/cm$^3$) and power density (i.e., 20.02 MW/MTU) were used to calculate the data for HCNGS assembly YJB732 burned to 37,570 MWd/MTU.

**Table 10. Behavior of Decay Heat as a Function of Initial Enrichment and Postirradiation Cooling Time**

| Initial Enrich. (wt % $^{235}$U) | Postirradiation Decay Time (years) | | | | | | |
|---|---|---|---|---|---|---|---|
| | 5 | 10 | 20 | 40 | 60 | 80 | 100 |
| | Decay Heat (kW / MTU) | | | | | | |
| 0.71 | 2.236 | 1.475 | 1.109 | 0.737 | 0.525 | 0.398 | 0.320 |
| 1.00 | 2.178 | 1.436 | 1.086 | 0.731 | 0.526 | 0.401 | 0.323 |
| 1.25 | 2.133 | 1.407 | 1.070 | 0.727 | 0.526 | 0.403 | 0.325 |
| 1.50 | 2.091 | 1.382 | 1.056 | 0.724 | 0.526 | 0.404 | 0.326 |
| 1.75 | 2.053 | 1.360 | 1.044 | 0.721 | 0.527 | 0.405 | 0.327 |
| 2.00 | 2.017 | 1.341 | 1.034 | 0.718 | 0.527 | 0.406 | 0.328 |
| 2.25 | 1.983 | 1.325 | 1.025 | 0.715 | 0.526 | 0.406 | 0.328 |
| 2.50 | 1.953 | 1.310 | 1.017 | 0.713 | 0.525 | 0.406 | 0.328 |
| 2.75 | 1.925 | 1.298 | 1.011 | 0.710 | 0.525 | 0.405 | 0.327 |
| 3.00 | 1.901 | 1.288 | 1.005 | 0.708 | 0.523 | 0.404 | 0.326 |
| 3.25 | 1.879 | 1.278 | 1.000 | 0.706 | 0.522 | 0.403 | 0.325 |
| 3.50 | 1.858 | 1.271 | 0.996 | 0.703 | 0.520 | 0.401 | 0.323 |
| 3.75 | 1.840 | 1.264 | 0.992 | 0.701 | 0.518 | 0.399 | 0.321 |
| 4.00 | 1.824 | 1.258 | 0.989 | 0.698 | 0.515 | 0.397 | 0.319 |
| 4.25 | 1.809 | 1.252 | 0.985 | 0.696 | 0.513 | 0.395 | 0.317 |
| 4.50 | 1.795 | 1.248 | 0.982 | 0.693 | 0.511 | 0.392 | 0.314 |
| 4.75 | 1.783 | 1.243 | 0.979 | 0.691 | 0.508 | 0.389 | 0.311 |
| 5.00 | 1.771 | 1.239 | 0.977 | 0.688 | 0.505 | 0.386 | 0.308 |

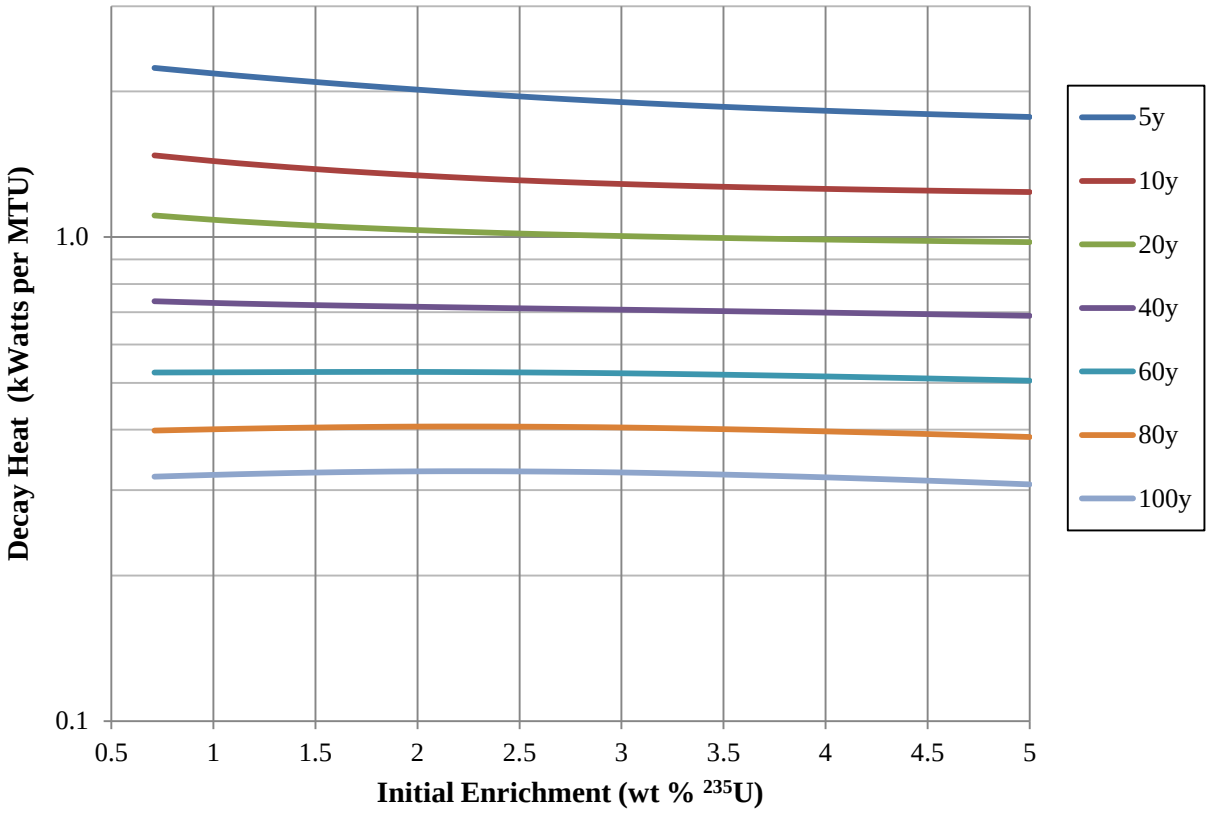


**Figure 6. Behavior of decay heat as a function of initial enrichment and postirradiation cooling time**

## 4.7 Impact of Computational Methods Used to Calculate Fuel Burnup and Decay Heat

This section provides results from studies designed to explore the impact of using various computational methods to calculate decay heat. Areas explored include the nuclides tracked in burned fuel composition calculations, depletion step size, DFs used in multigroup lattice calculations, use of alternative computer codes to calculate burnup dependent fluxes, and use of the ORIGAMI code.

### 4.7.1 Nuclides Tracked in Burned Fuel Composition Calculations

When radioactive nuclides decay, they produce daughter products or undergo spontaneous fission and can emit alpha particles ($^{+2}$He), electrons ($^{-}\beta$), neutrons, and/or gamma ($\gamma$) radiation. In the case of spontaneous fission, they may also produce fission products. The decay products leave the reaction with some energy, most of which is deposited locally as thermal energy, which is referred to as "decay heat." Due to time-dependent and locally varying conditions in the reactor, the variation in postirradiation cooling time, and the variation in radioactive nuclide decay half-lives, the set of nuclides important to decay heat determination varies. Table 11 shows the top 40 nuclides responsible for the decay heat generated by a 3 wt % $^{235}$U GE 8×8 assembly burned to 40 GWd/MTU and allowed to cool for various numbers of years. The table also shows which of the top nuclides are required to produce at least 99.9% of the total decay heat. Table 11 was produced using the SCALE 6.1 OrigenArp graphical user interface and the GE8×8–4 BWR ORIGEN library distributed with SCALE 6.1. These results are provided in this report purely to support identification of the nuclides important to decay heat generation.

**Table 11. Primary Decay Heat Contributors at Various Decay Times**

| 10 Year Decay Time | | | | 50 Year Decay Time | | | | 100 Year Decay Time | | | |
|---|---|---|---|---|---|---|---|---|---|---|---|
| Nuclide | Watts per MTU | % of total | Cum. % of total | Nuclide | Watts per MTU | % of total | Cum. % of total | Nuclide | Watts per MTU | % of total | Cum. % of total |
| $^{137m}$Ba | 368.1 | 27.22 | 27.22 | $^{137m}$Ba | 146.1 | 23.63 | 23.63 | $^{241}$Am | 122.9 | 38.36 | 38.36 |
| $^{90}$Y | 363.3 | 26.87 | 54.09 | $^{90}$Y | 135.7 | 21.95 | 45.58 | $^{238}$Pu | 56.61 | 17.67 | 56.03 |
| $^{244}$Cm | 123.8 | 9.15 | 63.24 | $^{241}$Am | 121.9 | 19.72 | 65.30 | $^{137m}$Ba | 46.00 | 14.36 | 70.38 |
| $^{238}$Pu | 115.1 | 8.51 | 71.75 | $^{238}$Pu | 83.95 | 13.58 | 78.88 | $^{90}$Y | 39.61 | 12.36 | 82.74 |
| $^{137}$Cs | 110.3 | 8.16 | 79.91 | $^{137}$Cs | 43.76 | 7.08 | 85.96 | $^{240}$Pu | 19.13 | 5.97 | 88.71 |
| $^{90}$Sr | 76.19 | 5.63 | 85.54 | $^{90}$Sr | 28.45 | 4.60 | 90.56 | $^{137}$Cs | 13.78 | 4.30 | 93.02 |
| $^{241}$Am | 57.47 | 4.25 | 89.79 | $^{244}$Cm | 26.75 | 4.33 | 94.89 | $^{90}$Sr | 8.305 | 2.59 | 95.61 |
| $^{134}$Cs | 57.14 | 4.23 | 94.02 | $^{240}$Pu | 19.17 | 3.10 | 97.99 | $^{239}$Pu | 8.268 | 2.58 | 98.19 |
| $^{154}$Eu | 27.93 | 2.07 | 96.08 | $^{239}$Pu | 8.278 | 1.34 | 99.33 | $^{244}$Cm | 3.942 | 1.23 | 99.42 |
| $^{240}$Pu | 19.02 | 1.41 | 97.49 | $^{243}$Am | 1.186 | 0.19 | 99.52 | $^{243}$Am | 1.180 | 0.37 | 99.79 |
| $^{239}$Pu | 8.285 | 0.61 | 98.10 | $^{154}$Eu | 1.108 | 0.18 | 99.70 | $^{242}$Cm | 0.194 | 0.06 | 99.85 |
| $^{85}$Kr | 8.122 | 0.60 | 98.70 | $^{85}$Kr | 0.611 | 0.10 | 99.80 | $^{239}$Np | 0.093 | 0.03 | 99.88 |
| $^{106}$Rh | 4.979 | 0.37 | 99.07 | $^{241}$Pu | 0.345 | 0.06 | 99.86 | $^{242}$Pu | 0.092 | 0.03 | 99.90 |
| $^{147}$Pm | 3.898 | 0.29 | 99.36 | $^{243}$Cm | 0.295 | 0.05 | 99.91 | $^{243}$Cm | 0.088 | 0.03 | 99.93 |
| $^{241}$Pu | 2.381 | 0.18 | 99.54 | $^{242}$Cm | 0.247 | 0.04 | 99.95 | $^{234}$U | 0.045 | 1.4E-02 | 99.95 |
| $^{125}$Sb | 2.045 | 0.15 | 99.69 | $^{239}$Np | 0.093 | 0.02 | 99.96 | $^{241}$Pu | 0.031 | 9.6E-03 | 99.96 |
| $^{243}$Am | 1.190 | 0.09 | 99.77 | $^{242}$Pu | 0.092 | 1.5E-02 | 99.98 | $^{85}$Kr | 0.0241 | 7.5E-03 | 99.96 |
| $^{243}$Cm | 0.781 | 0.06 | 99.83 | $^{234}$U | 0.037 | 6.0E-03 | 99.98 | $^{154}$Eu | 2.0E-02 | 6.1E-03 | 99.97 |
| $^{144}$Pr | 0.729 | 0.05 | 99.89 | $^{151}$Sm | 0.026 | 4.1E-03 | 99.99 | $^{151}$Sm | 1.7E-02 | 5.4E-03 | 99.97 |
| $^{155}$Eu | 0.630 | 0.05 | 99.93 | $^{245}$Cm | 1.2E-02 | 1.9E-03 | 99.99 | $^{237}$Np | 1.2E-02 | 3.8E-03 | 99.98 |
| $^{242}$Cm | 0.302 | 0.022 | 99.96 | $^{237}$Np | 1.0E-02 | 1.7E-03 | 99.99 | $^{245}$Cm | 1.2E-02 | 3.7E-03 | 99.98 |
| $^{125m}$Te | 0.133 | 9.8E-03 | 99.97 | $^{242}$Am | 9.4E-03 | 1.5E-03 | 99.99 | $^{126m}$Sb | 8.6E-03 | 2.7E-03 | 99.99 |
| $^{239}$Np | 0.093 | 6.9E-03 | 99.97 | $^{126m}$Sb | 8.6E-03 | 1.4E-03 | 99.99 | $^{99}$Tc | 8.0E-03 | 2.5E-03 | 99.99 |
| $^{242}$Pu | 0.092 | 6.8E-03 | 99.98 | $^{99}$Tc | 8.0E-03 | 1.3E-03 | 99.99 | $^{238}$U | 8.0E-03 | 2.5E-03 | 99.99 |
| $^{144}$Ce | 0.065 | 4.8E-03 | 99.98 | $^{238}$U | 8.0E-03 | 1.3E-03 | 99.99 | $^{236}$U | 7.5E-03 | 2.3E-03 | 99.99 |
| $^{151}$Sm | 0.035 | 2.6E-03 | 99.99 | $^{236}$U | 7.4E-03 | 1.2E-03 | 100.00 | $^{242}$Am | 7.4E-03 | 2.3E-03 | 99.99 |
| $^{152}$Eu | 0.033 | 2.4E-03 | 99.99 | $^{121}$Sn | 4.6E-03 | 7.4E-04 | 100.00 | $^{246}$Cm | 3.4E-03 | 1.1E-03 | 100.00 |
| $^{106}$Ru | 0.031 | 2.3E-03 | 99.99 | $^{152}$Eu | 4.1E-03 | 6.7E-04 | 100.00 | $^{242m}$Am | 2.6E-03 | 8.1E-04 | 100.00 |
| $^{234}$U | 0.027 | 2.0E-03 | 99.99 | $^{246}$Cm | 3.4E-03 | 5.5E-04 | 100.00 | $^{121}$Sn | 2.4E-03 | 7.6E-04 | 100.00 |
| $^{3}$H | 1.4E-02 | 1.0E-03 | 99.99 | $^{242m}$Am | 3.3E-03 | 5.4E-04 | 100.00 | $^{126}$Sb | 1.7E-03 | 5.4E-04 | 100.00 |
| $^{245}$Cm | 1.2E-02 | 8.9E-04 | 99.99 | $^{121m}$Sn | 2.0E-03 | 3.2E-04 | 100.00 | $^{234m}$Pa | 1.6E-03 | 4.8E-04 | 100.00 |
| $^{242}$Am | 1.2E-02 | 8.5E-04 | 100.00 | $^{126}$Sb | 1.7E-03 | 2.8E-04 | 100.00 | $^{233}$Pa | 1.1E-03 | 3.4E-04 | 100.00 |
| $^{237}$Np | 9.4E-03 | 6.9E-04 | 100.00 | $^{155}$Eu | 1.7E-03 | 2.7E-04 | 100.00 | $^{121m}$Sn | 1.1E-03 | 3.3E-04 | 100.00 |
| $^{126m}$Sb | 8.6E-03 | 6.4E-04 | 100.00 | $^{234m}$Pa | 1.6E-03 | 2.5E-04 | 100.00 | $^{126}$Sn | 1.0E-03 | 3.2E-04 | 100.00 |
| $^{99}$Tc | 8.0E-03 | 6.0E-04 | 100.00 | $^{3}$H | 1.4E-03 | 2.3E-04 | 100.00 | $^{216}$Po | 4.2E-04 | 1.3E-04 | 100.00 |
| $^{238}$U | 8.0E-03 | 5.9E-04 | 100.00 | $^{126}$Sn | 1.0E-03 | 1.7E-04 | 100.00 | $^{220}$Rn | 3.9E-04 | 1.2E-04 | 100.00 |
| $^{121}$Sn | 7.6E-03 | 5.6E-04 | 100.00 | $^{233}$Pa | 9.3E-04 | 1.5E-04 | 100.00 | $^{93m}$Nb | 3.5E-04 | 1.1E-04 | 100.00 |
| $^{236}$U | 7.4E-03 | 5.5E-04 | 100.00 | $^{216}$Po | 6.8E-04 | 1.1E-04 | 100.00 | $^{224}$Ra | 3.5E-04 | 1.1E-04 | 100.00 |
| $^{242m}$Am | 4.1E-03 | 3.0E-04 | 100.00 | $^{220}$Rn | 6.3E-04 | 1.0E-04 | 100.00 | $^{212}$Po | 3.4E-04 | 1.1E-04 | 100.00 |
| $^{237}$U | 3.5E-03 | 2.6E-04 | 100.00 | $^{224}$Ra | 5.7E-04 | 9.3E-05 | 100.00 | $^{228}$Th | 3.3E-04 | 1.0E-04 | 100.00 |
| Total | 1352.3 | | | Total | 618.19 | | | Total | 320.41 | | |

ORIGEN uses initial fuel compositions specified by the user and fluxes derived from the neutron transport calculation to calculate the compositions for all 2226 of the nuclides supported by ORIGEN. The burned-fuel compositions calculated by ORIGEN for the end of the depletion step are then returned

to the neutron transport calculation for recalculation of neutron fluxes. This cycle is repeated for each depletion step until the user-specified maximum burnup is achieved. The nuclides provided in the burned-fuel compositions passed from ORIGEN to the neutron transport code are limited to the set specified by the user in the TRITON input via the "addnux" input.

The fuel depletion sequences in the SCALE computer code system require the user to specify which set of nuclides to use during resonance self-shielding and neutron transport calculations. The options are described in Section T1.3.7.5 of Ref. 3. As is described in the reference, each addnux set specified in the reference is in addition to the preceding set or sets (i.e., addnux set 2 includes addnux sets 1 and -2). The addnux sets 1, -2, 2, 3 and 4 include 15, 64, 94, 230, and 388 nuclides, respectively.

The nuclide set specified using the "addnux" input affects only the neutron transport calculation. Use of different addnux values affects decay heat only through the neutron fluxes generated in the neutron transport calculations. The addnux input does not affect which nuclides are tracked by ORIGEN. Sensitivity calculations were performed with the various nuclide sets to explore the impact on the decay heat calculations. The results for HCNGS assembly YJB732 are presented in Table 12.

**Table 12. Effects of Various "addnux" Options on Calculated Decay Heat**

| | 5 Year Cooling Time | | | 11.8 Year Cooling Time | | | 50 year Cooling Time | | |
|---|---|---|---|---|---|---|---|---|---|
| addnux value | Decay Heat (kW/MTU) | Diff. from Ref. (%) | Runtime (hours) | Decay Heat (kW/MTU) | Diff. from Ref. (%) | Runtime (hours) | Decay Heat (kW/MTU) | Diff. from Ref. (%) | Runtime (hours) |
| 1 | 0.30922 | 1.9 | 11.0 | 0.21637 | 0.8 | 11.1 | 0.11207 | -1.5 | 11.3 |
| -2 | 0.30361 | 0.0 | 13.0 | 0.21468 | 0.0 | 13.1 | 0.11368 | -0.1 | 13.4 |
| 2 | 0.30356 | 0.0 | 14.5 | 0.21467 | 0.0 | 14.8 | 0.11376 | 0.0 | 15.2 |
| 3 | 0.30356 | Ref. | 21.4 | 0.21463 | Ref. | 45.1 | 0.11377 | Ref. | 23.0 |

From the results presented in Table 12, the results for addnux = 2 are nearly identical to the addnux = 3 results and required significantly less computer run time. In fact, the addnux = -2 results are also very close to the reference results. Use of the addnux = 2 option adds 30 nuclides compared to the -2 option and increases computer run time only modestly. The addnux = 4 option would add 158 nuclides compared to the addnux = 3 option, would increase memory and run time requirements significantly, and is expected to have no effect on the calculated decay heat. The addnux = 4 option was not available on the computer system used for this sensitivity study.

It is recommended that the addnux = 2 set be used for all decay heat calculations.

### 4.7.2 Depletion Time Step Size

Due to the iterative nature of the burned fuel composition calculations, the very broad range of radioactive nuclide half-lives involved, and the nature of the decay chains involved, the accuracy of the depletion calculations can be significantly affected by the size of the time step used between burned fuel composition calculations.

The depletion step size is set by a combination of the variables set in the "BURNDATA" input block described in Section T1.3.3.1 of Ref. 3. The user specifies the power density (power=), the number days to burn the fuel (burn=) at the specified power density, and the number of intervals into which the burnup is to be divided (nlib=). ORIGEN prepares nuclear data at interval midpoints for use in calculating the burned fuel compositions at the end of each interval. Figure 7 shows the TRITON BURNDATA input for HCNGS assembly YJB732 axial node 15.

```
read burndata
   power=37.345   burn=5      down=0      nlib=1   end
   power=37.345   burn=10     down=0      nlib=1   end
   power=37.345   burn=20     down=0      nlib=1   end
   power=37.345   burn=506.   down=81.    nlib=9   end

   power=31.402   burn=5      down=0      nlib=1   end
   power=31.402   burn=10     down=0      nlib=1   end
   power=31.402   burn=20     down=0      nlib=1   end
   power=31.402   burn=405.   down=45.    nlib=7   end

   power=18.048   burn=5      down=0      nlib=1   end
   power=18.048   burn=10     down=0      nlib=1   end
   power=18.048   burn=20     down=0      nlib=1   end
   power=18.048   burn=354.   down=30.    nlib=6   end

   power=8.464    burn=5      down=0      nlib=1   end
   power=8.464    burn=10     down=0      nlib=1   end
   power=8.464    burn=20     down=0      nlib=1   end
   power=8.464    burn=472.   down=4312    nlib=8   end

 end burndata
```

**Figure 7. Example of TRITON BURNDATA Input**

In this example, the power density is set to the cycle average value for each of four cycles and depleted for the actual number of days the cycle operated. Additional, smaller time steps are included at the beginning of each cycle to accurately model the early-cycle behavior of xenon and samarium and their impact on the neutron flux. It is appropriate to use longer time steps within each cycle after the xenon and samarium concentrations have reached near-equilibrium values. The fourth line in the first cycle burns the fuel at 37.345 MW/MTU for 506 days and then lets the fuel decay at zero power for 81 days. The 506 day burnup interval is divided into nine intervals of 56.2 days per interval. Neutron fluxes are calculated by NEWT at zero burnup in the first cycle, and then compositions and neutron fluxes are calculated by NEWT and ORIGEN at the midpoint of each interval, and a final set of compositions and decay heat are calculated by ORIGEN at the end of the final decay period.

The size of each depletion step is set by the length of the burnup interval divided by the number of subintervals requested via the nlib input. In this example, the nlib value was set such that the subintervals would be about 60 days.

Sensitivity studies were performed for HCNGS assembly YJB732 node 15 with nlib modified to yield approximately 30, 60, 100, 150, 200, and 400 day depletion intervals. The results are presented in Table 13. These calculations are all for YJB732 node 15 burned to 45.3 GWd/MTU and following an 11.8 year postirradiation cooling time.

**Table 13. Depletion Time Step Size Study**

| Average Time Step (days) | Decay Heat (kW/MTU) | Diff. from Ref. (%) | Run Time (hours) |
|---|---|---|---|
| 29 | 1.5141 | -0.02 | 19.7 |
| 58 | 1.5144 | Ref. | 11.1 |
| 97 | 1.5178 | 0.20 | 8.2 |
| 158 | 1.5194 | 0.33 | 7.4 |
| 193 | 1.5193 | 0.32 | 6.8 |
| 434 | 1.5206 | 0.41 | 6.3 |

From the data in Table 13, it appears that there is no benefit to using time steps smaller than about 60 days. Provided a few smaller time steps are taken early in the cycle to establish equilibrium xenon and samarium, using a single depletion step for the remainder of each cycle appears to have minimal impact on the calculated decay heat. The final case utilized a value of 1 for all "nlib" entries in Figure 7. Depending on how the decay heat value is used, this approach may be acceptable and is relatively fast compared to the reference case values, which are shown in Figure 7.

### 4.7.3 Dancoff Factors Used in Multigroup Lattice Calculations

The TRITON calculations utilizing multigroup cross sections require resonance self-shielding calculations to accurately calculate the effects of neutron absorption in cross-section resonances. This resonance absorption is important to decay heat calculations because neutron absorption in $^{238}U$ is the path by which plutonium and the other higher actinides are formed. A commonly used analysis approach is to perform resonance self-shielding calculations assuming that the fuel pin is in an infinite lattice of identical fuel pins. In SCALE, the resonance self-shielding associated with neighboring fuel pins is accounted for using DFs. This is described in Section M7.2.5 of the SCALE 6.1 Manual [3]. The reference case results for HCNGS assembly YJB732 utilized the standard infinite lattice treatment. Particularly for large fuel bundles, this is not a bad approximation. However, BWR fuel bundles are relatively small compared to pressurized water reactor bundles and it may be necessary to account for the decreased resonance self-shielding in fuel pins on the perimeter of each bundle.

SCALE includes the abilities to calculate and use fuel-rod-specific resonance self-shielding factors. These fuel-rod-specific DFs can be calculated using the SCALE MCDANCOFF program documented in Section M24 of the SCALE 6.1 manual [3]. A sensitivity study was performed to examine the impact of using a more detailed treatment of problem-specific resonance self-shielding on decay heat calculations for BWR fuel bundles. The DFs vary with both rod position and moderator density. In the study, DFs calculated for interior, side, and corner fuel pins were used in decay heat calculations for three of the axial zones in HCNGS assembly YJB732. The results are presented in Table 14.

From the results in Table 14, it appears that explicit modeling of pin-by-pin DFs may result in calculated decay heat values being as much as 2% higher. It is recommended that, where accurate decay heat values are needed, DFs for interior, side, and corner pins be modeled explicitly or that additional studies be performed justifying use of the infinite lattice DFs. These results are from HCNGS assembly YJB732 burned to an assembly average burnup of 37.6 GWd/MTU and following a postirradiation cooling time of 11.8 years.

**Table 14. Impact of Using Pin-by-Pin Dancoff Factors**

| Axial Node | Water Density ($g/cm^3$) | Decay Heat (kW/MTU) | | Difference from Ref. (%) | Difference from Ref. (kW/MTU) |
|---|---|---|---|---|---|
| | | Infinite-Lattice DFs, "Ref." | Pin-Specific DFs | | |
| 23 | 0.14845 | 0.8573 | 0.8721 | 1.7 | 0.0148 |
| 15 | 0.22487 | 1.5141 | 1.5173 | 0.2 | 0.0032 |
| 2 | 0.75408 | 0.8213 | 0.8215 | 0.0 | 0.0002 |

### 4.7.4 Axial Decay Heat Profile Modeling

As was noted in the preceding section, the power density varies axially. Integration of the axially varying power density over time yields the accumulated fuel burnup, typically discussed in units of megawatt-days or gigawatt-days per metric ton of uranium. Consequently, the axial slice burnup and decay heat vary axially. Rather than calculating the axially dependent decay heat explicitly, one might approximate the distribution by applying the normalized axial burnup profile to the assembly average decay heat. Table 15 shows the decay heat calculated for HCNGS assembly YJB732 and the decay heat approximated using the combination of the average decay heat and the normalized axial burnup profile. The results show that using the axial burnup shape to approximate the axial decay heat distribution can lead to significant errors, particularly near the top and bottom of an assembly.

**Table 15. Approximating Axial Distribution of Decay Heat for YJB732**

| Axial Node | Decay Heat (kW/MTU) | Axial Node Burnup (MWd/MTU) | Normalized | Approximate Decay Heat (kW/MTU) | Diff. (%) |
|---|---|---|---|---|---|
| 25 | 0.199 | 7149 | 0.190 | 0.229 | 15.2 |
| 24 | 0.329 | 11484 | 0.306 | 0.368 | 11.6 |
| 23 | 0.857 | 27912 | 0.743 | 0.894 | 4.2 |
| 22 | 1.090 | 34232 | 0.911 | 1.096 | 0.5 |
| 21 | 1.254 | 38408 | 1.022 | 1.230 | -1.9 |
| 20 | 1.372 | 41490 | 1.104 | 1.328 | -3.2 |
| 19 | 1.440 | 43180 | 1.149 | 1.383 | -4.0 |
| 18 | 1.474 | 44062 | 1.173 | 1.411 | -4.3 |
| 17 | 1.489 | 44501 | 1.184 | 1.425 | -4.3 |
| 16 | 1.508 | 45048 | 1.199 | 1.442 | -4.3 |
| 15 | 1.514 | 45333 | 1.207 | 1.451 | -4.1 |
| 14 | 1.513 | 45440 | 1.209 | 1.455 | -3.8 |
| 13 | 1.520 | 45774 | 1.218 | 1.466 | -3.6 |
| 12 | 1.513 | 45823 | 1.220 | 1.467 | -3.0 |
| 11 | 1.498 | 45692 | 1.216 | 1.463 | -2.4 |
| 10 | 1.433 | 44223 | 1.177 | 1.416 | -1.2 |
| 9 | 1.416 | 44076 | 1.173 | 1.411 | -0.3 |
| 8 | 1.390 | 43758 | 1.165 | 1.401 | 0.8 |
| 7 | 1.358 | 43269 | 1.152 | 1.385 | 2.1 |
| 6 | 1.331 | 42975 | 1.144 | 1.376 | 3.4 |
| 5 | 1.285 | 42169 | 1.122 | 1.350 | 5.1 |
| 4 | 1.209 | 40479 | 1.077 | 1.296 | 7.2 |
| 3 | 1.084 | 37174 | 0.989 | 1.190 | 9.8 |
| 2 | 0.821 | 28982 | 0.771 | 0.928 | 13.0 |
| 1 | 0.177 | 6654 | 0.177 | 0.213 | 20.5 |
| Average | 1.203 | 37571 | 1.000 | 1.203 | |

### 4.7.5 ORIGAMI

ORIGAMI, a new sequence distributed with SCALE in version 6.2, uses pregenerated problem-specific ORIGEN libraries and the ORIGEN code [Section F7 in Ref. 3] to rapidly perform burned fuel composition calculations. The products of the ORIGAMI calculations can include burned fuel compositions for use in criticality calculations, radiation source information for use in radiation dose calculations, and the decay heat source terms associated with the decay of the radioactive components of the burned nuclear fuel.

The primary benefit of using ORIGAMI is that it is much faster and requires very modest computing equipment. Consequently, ORIGAMI calculations can be tailored to provide a more realistic assembly-specific fuel depletion simulation.

As was discussed in Section 2.2.5, a drawback to using ORIGAMI and similar methods (i.e., ORIGEN-ARP, described in Section D1 of Ref. 3) is that many reactor depletion parameter values and fuel assembly design variations are included implicitly in the problem-specific ORIGEN library. This shortcoming may be overcome by generating a wide variety of ORIGEN libraries to cover the parameter space of interest.

The remainder of this section provides comparisons of decay heat calculation results from the HCNGS reference calculations and from ORIGAMI calculations.

The fuel assemblies in the HCNGS analysis were all GE7 and GE9 BWR fuel assembly designs, which are 8×8 lattices. Two of the fuel rods are replaced with two small water rods in the GE7 design (see Figure 1) and four fuel rods are replaced with one large water rod in the GE9 design.

Three ORIGEN libraries were used in ORIGAMI calculations to generate decay heat information for comparison with the HCNGS reference results. All three libraries were for BWR fuel bundles that were 8 rows by 8 columns of fuel pins on a 1.6256 cm center-to-center spacing. SCALE 6.1.3 library GE8×8–4 and two libraries generated in support of UFD work, referred to as the nominal and bounding versions of ORIGEN library G4608G4b, were used for the ORIGAMI calculations reported in this section. Table 16 shows a comparison of the HCNGS decay heat calculation models with the models used to generate the ORIGEN libraries used in the ORIGAMI calculations.

**Table 16. Comparison of HCNGS DH Models with ORIGEN Library Models**

| Fuel Assembly Model | | | | | |
|---|---|---|---|---|---|
| Library name | n/a | n/a | GE8×8–4 | G4608G4B | G4608G4B |
| Reference | HCNGS | | 3 | 15, nominal | 15, bounding |
| Fuel Assembly Design | GE7 | GE9 | GE9 | GE-4B | GE-4B |
| Fuel Pellet OD (cm) | 1.0566 | 1.0439 | 1.0566 | 1.05664 | 1.05664 |
| $UO_2$ Density (g/cm$^3$) | 10.5216 | 10.5216 | 9.863 | 10.32 | 10.741 |
| $Gd_2O_3$ Loading in Gd Rods (wt | 4 | 4 | 3 | 3 | 3 |
| $UO_2$+$Gd_2O_3$ Density (g/cm$^3$) | 10.5216 | 10.5216 | 9.863 | 10.32 | 10.741 |
| Fuel Rod Clad ID (cm) | 1.0795 | 1.0643 | 1.0642 | 1.0795 | 1.0795 |
| Fuel Rod Clad OD (cm) | 1.2268 | 1.2268 | 1.2268 | 1.25222 | 1.25222 |
| Fuel Rod Clad material | zirc-2 | zirc-2 | zirc-2 | zirc-2 | zirc-2 |
| Water Rod ID (cm) | 1.3487 | 3.2004 | 3.2004 | 1.0795 | 1.0795 |
| Water Rod OD (cm) | 1.5011 | 3.4036 | 3.4036 | 1.25222 | 1.25222 |
| Water Rod Tube Material | zirc-2 | zirc-2 | zirc-4 | zirc-4 | zirc-4 |
| Number of Fuel Rods | 53 | 51 | 51 | 58 | 58 |
| Number of $Gd_2O_3$ rods | 9 | 9 | 9 | 5 | 5 |
| Number of Water Rods | 2 | 1 | 1 | 1 | 1 |
| Fuel Rod Pitch (cm) | 1.6256 | 1.6256 | 1.6256 | 1.6256 | 1.6256 |
| Fuel Channel ID (cm) | 13.4061 | 13.4061 | 13.0048 | 13.2048 | 13.2048 |
| Fuel Channel Thickness (cm) | 0.2032 | 0.2032 | 0.2032 | 0.2032 | 0.2032 |
| Reactor Model | | | | | |
| Fuel Assembly Pitch (cm) | 15.24 | 15.24` | 15.1032 | 15.24 | 15.24 |
| Power Density (MW/MTU) | varied | varied | 40 | 25 | 25 |
| Fuel Temperature (K) | 1000 | 1000 | 1128.2 | 840 | 1200 |
| Moderator Density (g/cm$^3$) | varied | varied | 0.1-0.9 | 0.1-0.8 | 0.3 |
| Bypass Flow Density (g/cm$^3$) | ~0.75 | ~0.75 | 0.7396 | 0.742 | 0.737 |
| Control Blade Modeled? | inserted | inserted | withdrawn | withdrawn | inserted |

In the HCNGS calculations, the density of the water around the fuel rods and the power densities were modeled using axially-dependent assembly-specific best-estimate data for each of 25 axial slices modeled for each assembly. The models used to generate the various ORIGEN libraries have different numbers of fuel rods and would have significantly different uranium loading. The ORIGAMI calculations performed for this study used these libraries together with the HCNGS uranium loadings to generate decay heat results that are directly comparable to the HCNGS decay heat results.

The ORIGAMI code has another limitation in addition to the limitations associated with reactor depletion conditions noted in Section 2.2.5. The detailed TRITON/NEWT calculations modeled the cycle-to-cycle variation of the density of the water around the fuel pins. ORIGAMI currently does not support modeling of cycle-to-cycle moderator density variation. Consequently, the moderator density was calculated as the burnup-weighted average of the values for that axial slice. This average value was calculated for each axial slice and was used for all cycles for that slice. The remainder of this subsection provides comparisons of results from detailed TRITON/NEWT calculations with results generated using ORIGAMI.

#### *4.7.5.1 HCNGS Assemblies YJB732, LYB665, LYD228, and LYW549*

Table 17 provides a comparison of the total decay heat calculated for four of the HCNGS fuel assemblies. The assemblies were selected to represent the range of fuel assemblies stored in two HCNGS casks. In general, the ORIGAMI UFD bounding library results are significantly higher than the detailed best-estimate results generated using the SCALE TRITON T-DEPL sequence, and the ORIGAMI results using the SCALE and UFD nominal library results are reasonably close to the detailed results. Tables 18 through 21 and Figures 8 through 11 show how the axially dependent results for each fuel assembly vary with the calculational approach and ORIGEN library.

**Table 17. Decay Heat Calculation Method Comparison**

| Assembly ID | YJB732 | LYB665 | LYD228 | LYW549 |
|---|---|---|---|---|
| Assembly Design | GE9 | GE7 | GE7 | GE9 |
| Average Enrichment (wt % $^{235}$U) | 3.23 | 0.71 | 2.48 | 3.24 |
| Final Burnup (GWd/MTU) | 37.6 | 2.7 | 23.1 | 39.9 |
| Postirradiation Decay Time (years) | 11.8 | 25.5 | 22.6 | 17.7 |
| Power Density Range (MW/MTU) | 1.1 to 38.7 | 0.8 to 5.9 | 1.7 to 22.3 | 3.8 to 33.8 |
| Moderator Density Range (g/cm$^3$) | 0.13 to 0.76 | 0.38 to 0.76 | 0.18 to 0.76 | 0.17 to 0.76 |
| TRITON/NEWT (W / Assembly) | 214.6 | 10.7 | 105.5 | 203.7 |
| ORIGAMI + SCALE ge8×8–4 | | | | |
| Decay Heat (W / Assembly) | 209.8 | 10.7 | 101.4 | 197.6 |
| Difference from TRITON/NEWT (% )[a] | -2.3 | 0.2 | -4.0 | -3.1 |
| ORIGAMI + UFD Nominal G4608G4B | | | | |
| Decay Heat (W / Assembly) | 215.5 | 10.8 | 102.8 | 202.4 |
| Difference from TRITON/NEWT (%) | 0.4 | 1.5 | -2.6 | -0.6 |
| ORIGAMI + UFD Bounding G4608G4B | | | | |
| Decay Heat (W / Assembly) | 237.7 | 11.5 | 114.2 | 227.5 |
| Difference from TRITON/NEWT (%) | 10.7 | 8.1 | 8.3 | 11.7 |

[a] (ORIGAMI – TRITON)*100% / TRITON

**Table 18. Comparison of ORIGAMI and Detailed TRITON T-DEPL Calculations for HCNGS Assembly YJB732**

| Axial Node | TRITON/NEWT (Ref.) | ORIGAMI SCALE 6.1 Library ge8×8–4 | | ORIGAMI UFD Library Nominal G4608G4B | | ORIGAMI UFD Library Bounding G4608G4B | |
|---|---|---|---|---|---|---|---|
| | Decay Heat (Watts) | Decay Heat (Watts) | Diff. from Ref. (%) | Decay Heat (Watts) | Diff. from Ref. (%) | Decay Heat (Watts) | Diff. from Ref. (%) |
| 25 | 1.42E+00 | 1.43E+00 | 0.8 | 1.43E+00 | 1.0 | 1.48E+00 | 4.3 |
| 24 | 2.35E+00 | 2.32E+00 | -1.1 | 2.36E+00 | 0.5 | 2.47E+00 | 5.2 |
| 23 | 6.12E+00 | 5.98E+00 | -2.3 | 6.14E+00 | 0.3 | 6.41E+00 | 4.8 |
| 22 | 7.78E+00 | 7.55E+00 | -2.9 | 7.82E+00 | 0.5 | 8.24E+00 | 5.9 |
| 21 | 8.95E+00 | 8.66E+00 | -3.2 | 9.01E+00 | 0.7 | 9.55E+00 | 6.7 |
| 20 | 9.79E+00 | 9.48E+00 | -3.2 | 9.87E+00 | 0.8 | 1.05E+01 | 7.1 |
| 19 | 1.03E+01 | 9.95E+00 | -3.2 | 1.04E+01 | 0.8 | 1.11E+01 | 7.5 |
| 18 | 1.05E+01 | 1.02E+01 | -3.2 | 1.06E+01 | 0.8 | 1.13E+01 | 7.9 |
| 17 | 1.06E+01 | 1.03E+01 | -3.1 | 1.07E+01 | 0.7 | 1.15E+01 | 8.2 |
| 16 | 1.08E+01 | 1.04E+01 | -3.0 | 1.08E+01 | 0.7 | 1.17E+01 | 8.6 |
| 15 | 1.08E+01 | 1.05E+01 | -3.0 | 1.09E+01 | 0.6 | 1.18E+01 | 9.0 |
| 14 | 1.08E+01 | 1.05E+01 | -2.9 | 1.09E+01 | 0.5 | 1.18E+01 | 9.4 |
| 13 | 1.08E+01 | 1.05E+01 | -2.8 | 1.09E+01 | 0.5 | 1.19E+01 | 9.9 |
| 12 | 1.08E+01 | 1.05E+01 | -2.6 | 1.08E+01 | 0.4 | 1.19E+01 | 10.5 |
| 11 | 1.07E+01 | 1.04E+01 | -2.5 | 1.07E+01 | 0.3 | 1.19E+01 | 11.2 |
| 10 | 1.02E+01 | 9.99E+00 | -2.3 | 1.03E+01 | 0.3 | 1.14E+01 | 11.9 |
| 9 | 1.01E+01 | 9.89E+00 | -2.1 | 1.01E+01 | 0.2 | 1.14E+01 | 12.7 |
| 8 | 9.92E+00 | 9.73E+00 | -1.9 | 9.94E+00 | 0.2 | 1.13E+01 | 13.6 |
| 7 | 9.69E+00 | 9.53E+00 | -1.7 | 9.70E+00 | 0.1 | 1.11E+01 | 14.6 |
| 6 | 9.50E+00 | 9.36E+00 | -1.4 | 9.50E+00 | 0.0 | 1.10E+01 | 15.6 |
| 5 | 9.17E+00 | 9.07E+00 | -1.2 | 9.17E+00 | 0.0 | 1.07E+01 | 16.7 |
| 4 | 8.63E+00 | 8.56E+00 | -0.8 | 8.62E+00 | -0.1 | 1.01E+01 | 17.5 |
| 3 | 7.74E+00 | 7.71E+00 | -0.4 | 7.73E+00 | 0.0 | 9.07E+00 | 17.3 |
| 2 | 5.86E+00 | 5.88E+00 | 0.3 | 5.88E+00 | 0.2 | 6.66E+00 | 13.6 |
| 1 | 1.26E+00 | 1.30E+00 | 3.3 | 1.28E+00 | 1.2 | 1.37E+00 | 8.4 |
| Total | 2.15E+02 | 2.10E+02 | -2.3 | 2.16E+02 | 0.4 | 2.38E+02 | 10.7 |

**Table 19. Comparison of ORIGAMI and Detailed TRITON T-DEPL Calculations for HCNGS Assembly YJB665**

| Axial Node | TRITON/NEWT (Ref.) | ORIGAMI SCALE 6.1 Library ge8×8–4 | | ORIGAMI UFD Library Nominal G4608G4B | | ORIGAMI UFD Library Bounding G4608G4B | |
|---|---|---|---|---|---|---|---|
| | Decay Heat (Watts) | Decay Heat (Watts) | Diff. from Ref. (%) | Decay Heat (Watts) | Diff. from Ref. (%) | Decay Heat (Watts) | Diff. from Ref. (%) |
| 25 | 9.36E-02 | 9.53E-02 | 1.8 | 9.64E-02 | 3.0 | 9.98E-02 | 6.6 |
| 24 | 1.69E-01 | 1.71E-01 | 1.5 | 1.74E-01 | 3.0 | 1.80E-01 | 6.4 |
| 23 | 2.51E-01 | 2.53E-01 | 0.9 | 2.57E-01 | 2.7 | 2.67E-01 | 6.4 |
| 22 | 3.23E-01 | 3.24E-01 | 0.4 | 3.30E-01 | 2.3 | 3.44E-01 | 6.6 |
| 21 | 3.85E-01 | 3.85E-01 | 0.1 | 3.92E-01 | 1.9 | 4.10E-01 | 6.7 |
| 20 | 4.35E-01 | 4.34E-01 | -0.1 | 4.41E-01 | 1.6 | 4.64E-01 | 6.8 |
| 19 | 4.80E-01 | 4.78E-01 | -0.3 | 4.86E-01 | 1.3 | 5.13E-01 | 7.0 |
| 18 | 5.13E-01 | 5.11E-01 | -0.4 | 5.19E-01 | 1.1 | 5.50E-01 | 7.2 |
| 17 | 5.33E-01 | 5.31E-01 | -0.4 | 5.39E-01 | 1.1 | 5.72E-01 | 7.4 |
| 16 | 5.51E-01 | 5.49E-01 | -0.4 | 5.56E-01 | 1.0 | 5.93E-01 | 7.6 |
| 15 | 5.60E-01 | 5.58E-01 | -0.3 | 5.65E-01 | 1.0 | 6.04E-01 | 7.8 |
| 14 | 5.63E-01 | 5.61E-01 | -0.2 | 5.68E-01 | 1.0 | 6.08E-01 | 8.0 |
| 13 | 5.71E-01 | 5.70E-01 | -0.2 | 5.76E-01 | 1.0 | 6.18E-01 | 8.2 |
| 12 | 5.72E-01 | 5.72E-01 | -0.1 | 5.78E-01 | 1.0 | 6.20E-01 | 8.5 |
| 11 | 5.66E-01 | 5.66E-01 | 0.1 | 5.72E-01 | 1.1 | 6.15E-01 | 8.7 |
| 10 | 5.54E-01 | 5.55E-01 | 0.2 | 5.60E-01 | 1.2 | 6.03E-01 | 8.9 |
| 9 | 5.47E-01 | 5.49E-01 | 0.3 | 5.54E-01 | 1.3 | 5.97E-01 | 9.1 |
| 8 | 5.36E-01 | 5.39E-01 | 0.4 | 5.44E-01 | 1.4 | 5.86E-01 | 9.3 |
| 7 | 5.18E-01 | 5.21E-01 | 0.5 | 5.26E-01 | 1.5 | 5.66E-01 | 9.3 |
| 6 | 4.98E-01 | 5.01E-01 | 0.6 | 5.06E-01 | 1.6 | 5.44E-01 | 9.3 |
| 5 | 4.60E-01 | 4.64E-01 | 0.7 | 4.68E-01 | 1.7 | 5.02E-01 | 9.1 |
| 4 | 3.97E-01 | 4.01E-01 | 1.0 | 4.05E-01 | 2.0 | 4.32E-01 | 8.8 |
| 3 | 3.13E-01 | 3.17E-01 | 1.4 | 3.20E-01 | 2.4 | 3.39E-01 | 8.3 |
| 2 | 1.98E-01 | 2.02E-01 | 1.9 | 2.03E-01 | 2.7 | 2.13E-01 | 7.4 |
| 1 | 7.15E-02 | 7.29E-02 | 2.0 | 7.32E-02 | 2.4 | 7.66E-02 | 7.2 |
| Total | 1.07E+01 | 1.07E+01 | 0.2 | 1.08E+01 | 1.5 | 1.15E+01 | 8.1 |

**Table 20. Comparison of ORIGAMI and Detailed TRITON T-DEPL Calculations for HCNGS Assembly LYD228**

| Axial Node | TRITON/NEWT (Ref.) | ORIGAMI SCALE 6.1 Library ge8×8–4 | | ORIGAMI UFD Library Nominal G4608G4B | | ORIGAMI UFD Library Bounding G4608G4B | |
|---|---|---|---|---|---|---|---|
| | Decay Heat (Watts) | Decay Heat (Watts) | Diff. from Ref. (%) | Decay Heat (Watts) | Diff. from Ref. (%) | Decay Heat (Watts) | Diff. from Ref. (%) |
| 25 | 8.34E-01 | 8.16E-01 | -2.2 | 8.33E-01 | -0.1 | 8.71E-01 | 4.4 |
| 24 | 2.26E+00 | 2.21E+00 | -2.4 | 2.22E+00 | -1.6 | 2.32E+00 | 2.6 |
| 23 | 3.14E+00 | 3.03E+00 | -3.7 | 3.07E+00 | -2.4 | 3.24E+00 | 2.9 |
| 22 | 3.83E+00 | 3.65E+00 | -4.6 | 3.72E+00 | -2.9 | 3.96E+00 | 3.4 |
| 21 | 4.29E+00 | 4.07E+00 | -5.1 | 4.16E+00 | -3.1 | 4.45E+00 | 3.8 |
| 20 | 4.60E+00 | 4.35E+00 | -5.4 | 4.45E+00 | -3.3 | 4.79E+00 | 4.2 |
| 19 | 4.84E+00 | 4.58E+00 | -5.5 | 4.68E+00 | -3.3 | 5.07E+00 | 4.6 |
| 18 | 5.01E+00 | 4.73E+00 | -5.6 | 4.84E+00 | -3.4 | 5.27E+00 | 5.0 |
| 17 | 5.10E+00 | 4.82E+00 | -5.5 | 4.93E+00 | -3.4 | 5.38E+00 | 5.5 |
| 16 | 5.17E+00 | 4.89E+00 | -5.4 | 4.99E+00 | -3.4 | 5.47E+00 | 5.9 |
| 15 | 5.20E+00 | 4.93E+00 | -5.2 | 5.03E+00 | -3.3 | 5.54E+00 | 6.5 |
| 14 | 5.21E+00 | 4.95E+00 | -5.0 | 5.04E+00 | -3.2 | 5.58E+00 | 7.1 |
| 13 | 5.27E+00 | 5.01E+00 | -4.8 | 5.10E+00 | -3.2 | 5.67E+00 | 7.8 |
| 12 | 5.26E+00 | 5.02E+00 | -4.6 | 5.10E+00 | -3.0 | 5.71E+00 | 8.5 |
| 11 | 5.24E+00 | 5.02E+00 | -4.3 | 5.09E+00 | -2.9 | 5.73E+00 | 9.3 |
| 10 | 5.17E+00 | 4.97E+00 | -3.9 | 5.03E+00 | -2.7 | 5.69E+00 | 10.1 |
| 9 | 5.10E+00 | 4.92E+00 | -3.5 | 4.97E+00 | -2.5 | 5.66E+00 | 11.1 |
| 8 | 5.03E+00 | 4.88E+00 | -3.1 | 4.92E+00 | -2.3 | 5.64E+00 | 12.0 |
| 7 | 4.91E+00 | 4.78E+00 | -2.6 | 4.81E+00 | -2.0 | 5.54E+00 | 12.9 |
| 6 | 4.75E+00 | 4.65E+00 | -2.2 | 4.67E+00 | -1.8 | 5.40E+00 | 13.7 |
| 5 | 4.50E+00 | 4.42E+00 | -1.7 | 4.43E+00 | -1.5 | 5.13E+00 | 14.1 |
| 4 | 4.10E+00 | 4.06E+00 | -1.1 | 4.06E+00 | -1.1 | 4.67E+00 | 13.9 |
| 3 | 3.56E+00 | 3.54E+00 | -0.5 | 3.53E+00 | -0.7 | 4.01E+00 | 12.7 |
| 2 | 2.52E+00 | 2.53E+00 | 0.4 | 2.51E+00 | -0.1 | 2.77E+00 | 10.1 |
| 1 | 5.66E-01 | 5.70E-01 | 0.8 | 5.74E-01 | 1.5 | 6.18E-01 | 9.2 |
| Total | 1.05E+02 | 1.01E+02 | -3.9 | 1.03E+02 | -2.6 | 1.14E+02 | 8.3 |

**Table 21. Comparison of ORIGAMI and Detailed TRITON T-DEPL Calculations for HCNGS Assembly LYW549**

| Axial Node | TRITON/NEWT (Ref.) | ORIGAMI SCALE 6.1 Library ge8×8–4 | | ORIGAMI UFD Library Nominal G4608G4B | | ORIGAMI UFD Library Bounding G4608G4B | |
|---|---|---|---|---|---|---|---|
| | Decay Heat (Watts) | Decay Heat (Watts) | Diff. from Ref. (%) | Decay Heat (Watts) | Diff. from Ref. (%) | Decay Heat (Watts) | Diff. from Ref. (%) |
| 25 | 1.51E+00 | 1.50E+00 | -1.2 | 1.51E+00 | 0.1 | 1.59E+00 | 4.8 |
| 24 | 2.33E+00 | 2.26E+00 | -2.7 | 2.31E+00 | -0.6 | 2.45E+00 | 5.5 |
| 23 | 5.62E+00 | 5.45E+00 | -3.0 | 5.59E+00 | -0.5 | 5.90E+00 | 4.9 |
| 22 | 7.05E+00 | 6.78E+00 | -3.8 | 7.01E+00 | -0.6 | 7.47E+00 | 6.0 |
| 21 | 8.12E+00 | 7.78E+00 | -4.1 | 8.07E+00 | -0.6 | 8.66E+00 | 6.7 |
| 20 | 8.88E+00 | 8.50E+00 | -4.2 | 8.83E+00 | -0.6 | 9.51E+00 | 7.2 |
| 19 | 9.39E+00 | 8.99E+00 | -4.2 | 9.33E+00 | -0.6 | 1.01E+01 | 7.6 |
| 18 | 9.75E+00 | 9.34E+00 | -4.2 | 9.69E+00 | -0.6 | 1.05E+01 | 8.0 |
| 17 | 1.00E+01 | 9.62E+00 | -4.1 | 9.97E+00 | -0.7 | 1.09E+01 | 8.4 |
| 16 | 1.03E+01 | 9.84E+00 | -4.0 | 1.02E+01 | -0.7 | 1.12E+01 | 8.9 |
| 15 | 1.04E+01 | 9.95E+00 | -3.9 | 1.03E+01 | -0.7 | 1.13E+01 | 9.4 |
| 14 | 1.04E+01 | 9.96E+00 | -3.8 | 1.03E+01 | -0.8 | 1.14E+01 | 9.9 |
| 13 | 1.04E+01 | 1.00E+01 | -3.6 | 1.03E+01 | -0.8 | 1.15E+01 | 10.5 |
| 12 | 1.04E+01 | 1.00E+01 | -3.5 | 1.03E+01 | -0.8 | 1.16E+01 | 11.3 |
| 11 | 1.03E+01 | 9.96E+00 | -3.3 | 1.02E+01 | -0.8 | 1.15E+01 | 12.1 |
| 10 | 1.01E+01 | 9.80E+00 | -3.0 | 1.00E+01 | -0.8 | 1.14E+01 | 13.0 |
| 9 | 9.98E+00 | 9.70E+00 | -2.8 | 9.90E+00 | -0.8 | 1.14E+01 | 14.0 |
| 8 | 9.52E+00 | 9.29E+00 | -2.5 | 9.45E+00 | -0.7 | 1.10E+01 | 15.2 |
| 7 | 9.24E+00 | 9.05E+00 | -2.1 | 9.18E+00 | -0.7 | 1.08E+01 | 16.4 |
| 6 | 9.06E+00 | 8.90E+00 | -1.8 | 9.00E+00 | -0.6 | 1.07E+01 | 17.8 |
| 5 | 8.76E+00 | 8.64E+00 | -1.4 | 8.71E+00 | -0.6 | 1.04E+01 | 19.1 |
| 4 | 8.22E+00 | 8.14E+00 | -1.0 | 8.19E+00 | -0.4 | 9.86E+00 | 20.0 |
| 3 | 7.32E+00 | 7.28E+00 | -0.5 | 7.30E+00 | -0.3 | 8.75E+00 | 19.5 |
| 2 | 5.48E+00 | 5.50E+00 | 0.3 | 5.49E+00 | 0.2 | 6.32E+00 | 15.2 |
| 1 | 1.23E+00 | 1.26E+00 | 2.2 | 1.25E+00 | 1.1 | 1.36E+00 | 10.1 |
| Total | 2.04E+02 | 1.98E+02 | -3.0 | 2.02E+02 | -0.6 | 2.27E+02 | 11.7 |

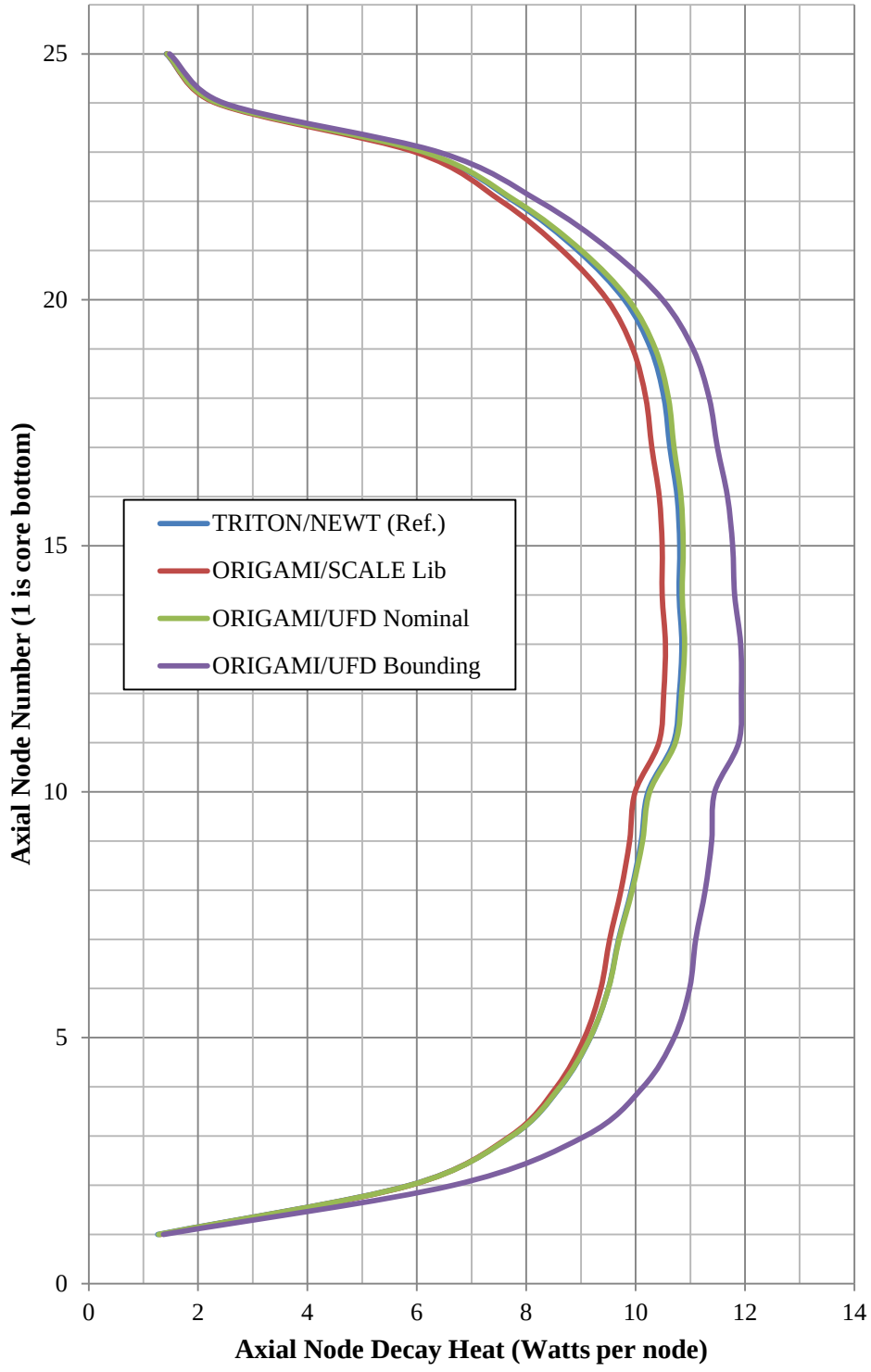


**Figure 8. Axially dependent decay heat results for HCNGS assembly YJB732**

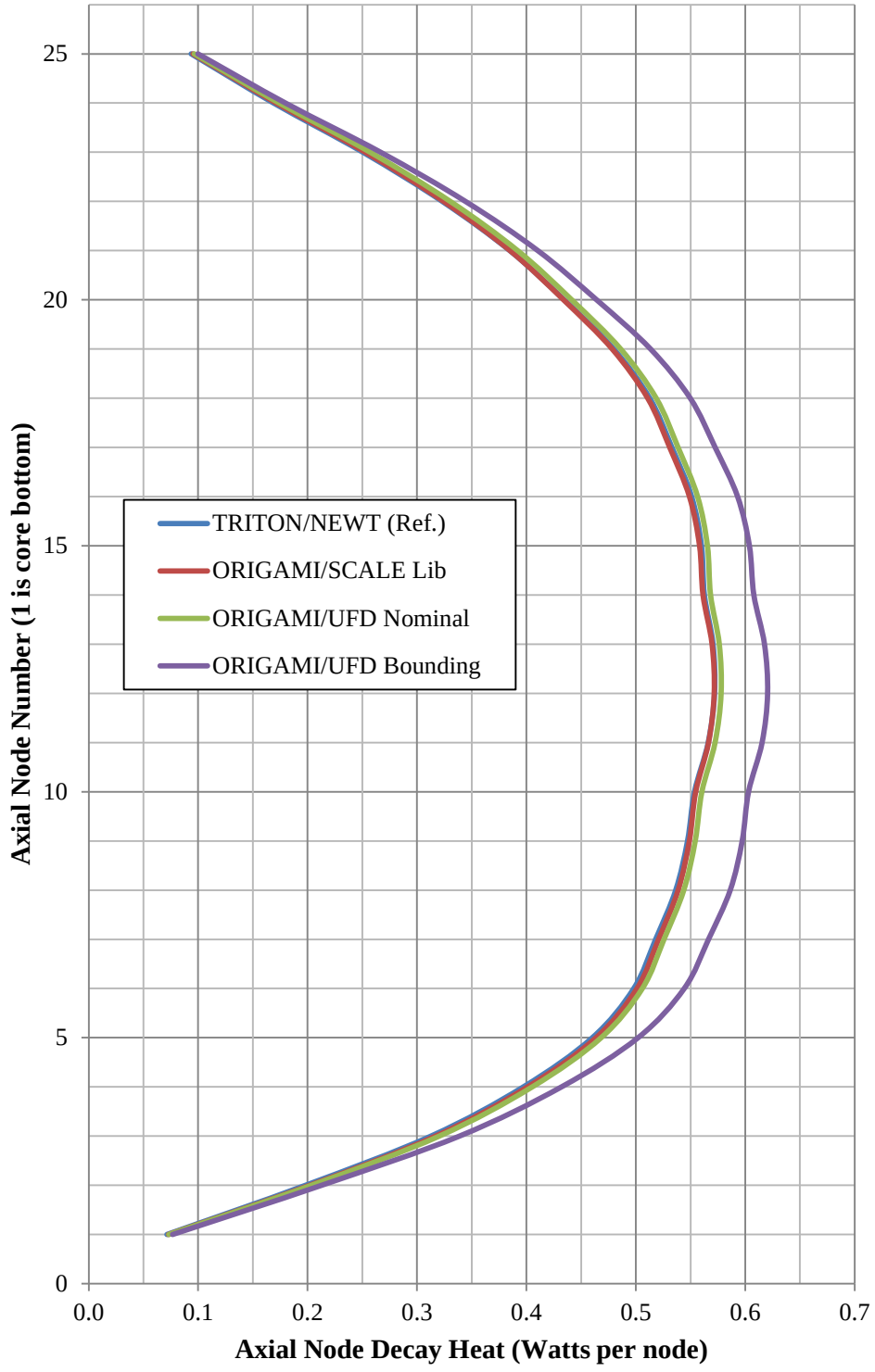


**Figure 9. Axially dependent decay heat results for HCNGS assembly LYB665**

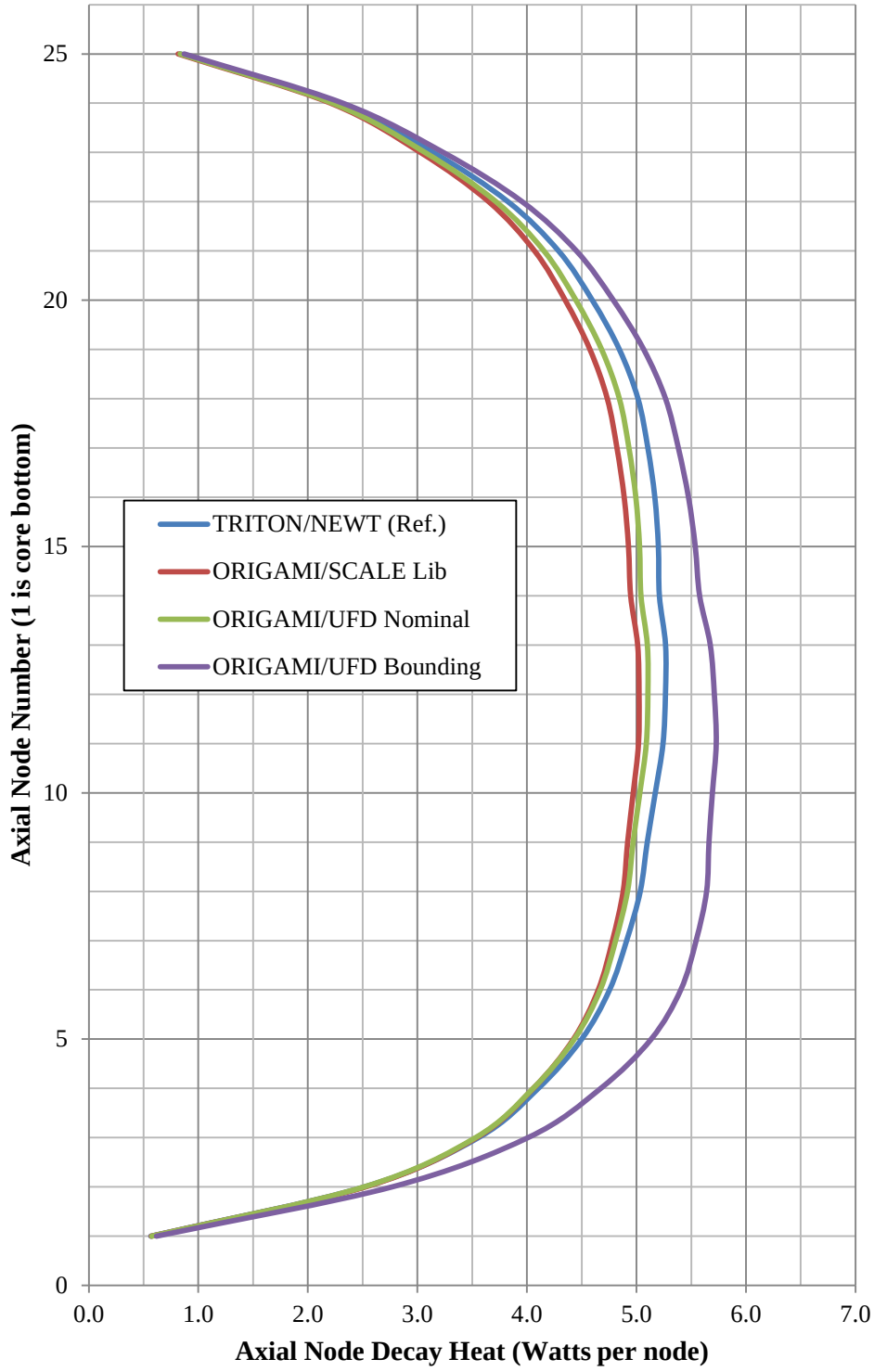


**Figure 10. Axially dependent decay heat results for HCNGS assembly LYD228**

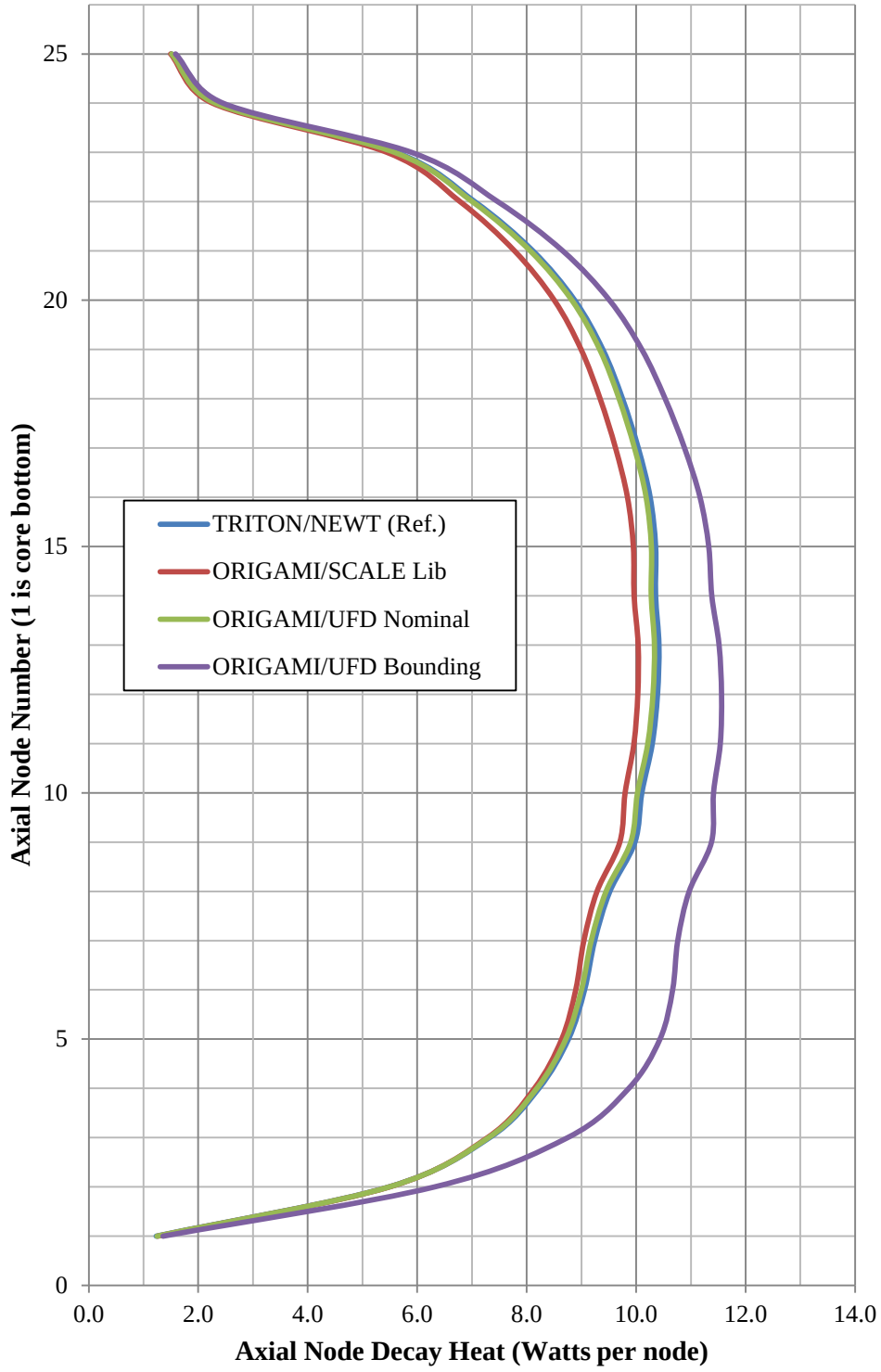


**Figure 11. Axially dependent decay heat results for HCNGS assembly LYW549**

#### *4.7.5.2 ORIGAMI Performance for Varying Postirradiation Decay Times*

Some additional detailed calculations were performed for HCNGS assembly YJB732 to provide a reference for comparison with ORIGAMI and varying postirradiation decay times. Table 22 and Figure 12 provide comparisons for YJB732 after only 5 years of decay time; Table 23 and Figure 13 show the comparison after 50 years of decay time.

**Table 22. Comparison of ORIGAMI and Detailed TRITON T-DEPL Calculations for HCNGS Assembly YJB732 with 5 Years of Decay Time**

| Axial Node | TRITON/NEWT (Ref.) | ORIGAMI SCALE 6.1 Library ge8×8–4 | | ORIGAMI UFD Library Nominal G4608G4B | | ORIGAMI UFD Library Bounding G4608G4B | |
|---|---|---|---|---|---|---|---|
| | Decay Heat (Watts) | Decay Heat (Watts) | Diff. from Ref. (%) | Decay Heat (Watts) | Diff. from Ref. (%) | Decay Heat (Watts) | Diff. from Ref. (%) |
| 25 | 1.85E+00 | 1.86E+00 | 0.4 | 1.88E+00 | 1.7 | 1.94E+00 | 4.6 |
| 24 | 3.17E+00 | 3.11E+00 | -2.0 | 3.23E+00 | 1.8 | 3.35E+00 | 5.7 |
| 23 | 8.49E+00 | 8.26E+00 | -2.7 | 8.61E+00 | 1.4 | 8.99E+00 | 5.9 |
| 22 | 1.09E+01 | 1.06E+01 | -3.2 | 1.12E+01 | 1.8 | 1.17E+01 | 7.0 |
| 21 | 1.27E+01 | 1.23E+01 | -3.2 | 1.29E+01 | 2.2 | 1.37E+01 | 7.7 |
| 20 | 1.39E+01 | 1.35E+01 | -3.3 | 1.42E+01 | 2.3 | 1.51E+01 | 8.1 |
| 19 | 1.46E+01 | 1.42E+01 | -3.2 | 1.50E+01 | 2.3 | 1.59E+01 | 8.4 |
| 18 | 1.50E+01 | 1.45E+01 | -3.2 | 1.53E+01 | 2.3 | 1.63E+01 | 8.7 |
| 17 | 1.52E+01 | 1.47E+01 | -3.1 | 1.55E+01 | 2.2 | 1.65E+01 | 9.0 |
| 16 | 1.54E+01 | 1.49E+01 | -3.0 | 1.57E+01 | 2.2 | 1.68E+01 | 9.4 |
| 15 | 1.54E+01 | 1.50E+01 | -3.0 | 1.58E+01 | 2.1 | 1.69E+01 | 9.8 |
| 14 | 1.54E+01 | 1.50E+01 | -2.9 | 1.57E+01 | 2.0 | 1.70E+01 | 10.2 |
| 13 | 1.55E+01 | 1.50E+01 | -2.8 | 1.58E+01 | 2.0 | 1.71E+01 | 10.6 |
| 12 | 1.54E+01 | 1.50E+01 | -2.7 | 1.57E+01 | 1.9 | 1.71E+01 | 11.2 |
| 11 | 1.52E+01 | 1.49E+01 | -2.6 | 1.55E+01 | 1.8 | 1.70E+01 | 11.8 |
| 10 | 1.46E+01 | 1.42E+01 | -2.4 | 1.48E+01 | 1.8 | 1.64E+01 | 12.5 |
| 9 | 1.44E+01 | 1.41E+01 | -2.2 | 1.46E+01 | 1.7 | 1.63E+01 | 13.2 |
| 8 | 1.41E+01 | 1.38E+01 | -2.1 | 1.43E+01 | 1.5 | 1.61E+01 | 14.0 |
| 7 | 1.37E+01 | 1.35E+01 | -1.9 | 1.39E+01 | 1.4 | 1.58E+01 | 14.9 |
| 6 | 1.34E+01 | 1.32E+01 | -1.7 | 1.36E+01 | 1.2 | 1.55E+01 | 15.9 |
| 5 | 1.29E+01 | 1.27E+01 | -1.5 | 1.30E+01 | 1.1 | 1.51E+01 | 16.9 |
| 4 | 1.20E+01 | 1.19E+01 | -1.2 | 1.22E+01 | 0.9 | 1.42E+01 | 17.8 |
| 3 | 1.07E+01 | 1.06E+01 | -0.9 | 1.08E+01 | 0.8 | 1.26E+01 | 17.8 |
| 2 | 7.93E+00 | 7.91E+00 | -0.3 | 8.00E+00 | 0.8 | 9.12E+00 | 15.0 |
| 1 | 1.63E+00 | 1.67E+00 | 2.3 | 1.66E+00 | 1.7 | 1.76E+00 | 7.9 |
| Total | 3.04E+02 | 2.96E+02 | -2.4 | 3.09E+02 | 1.8 | 3.38E+02 | 11.4 |

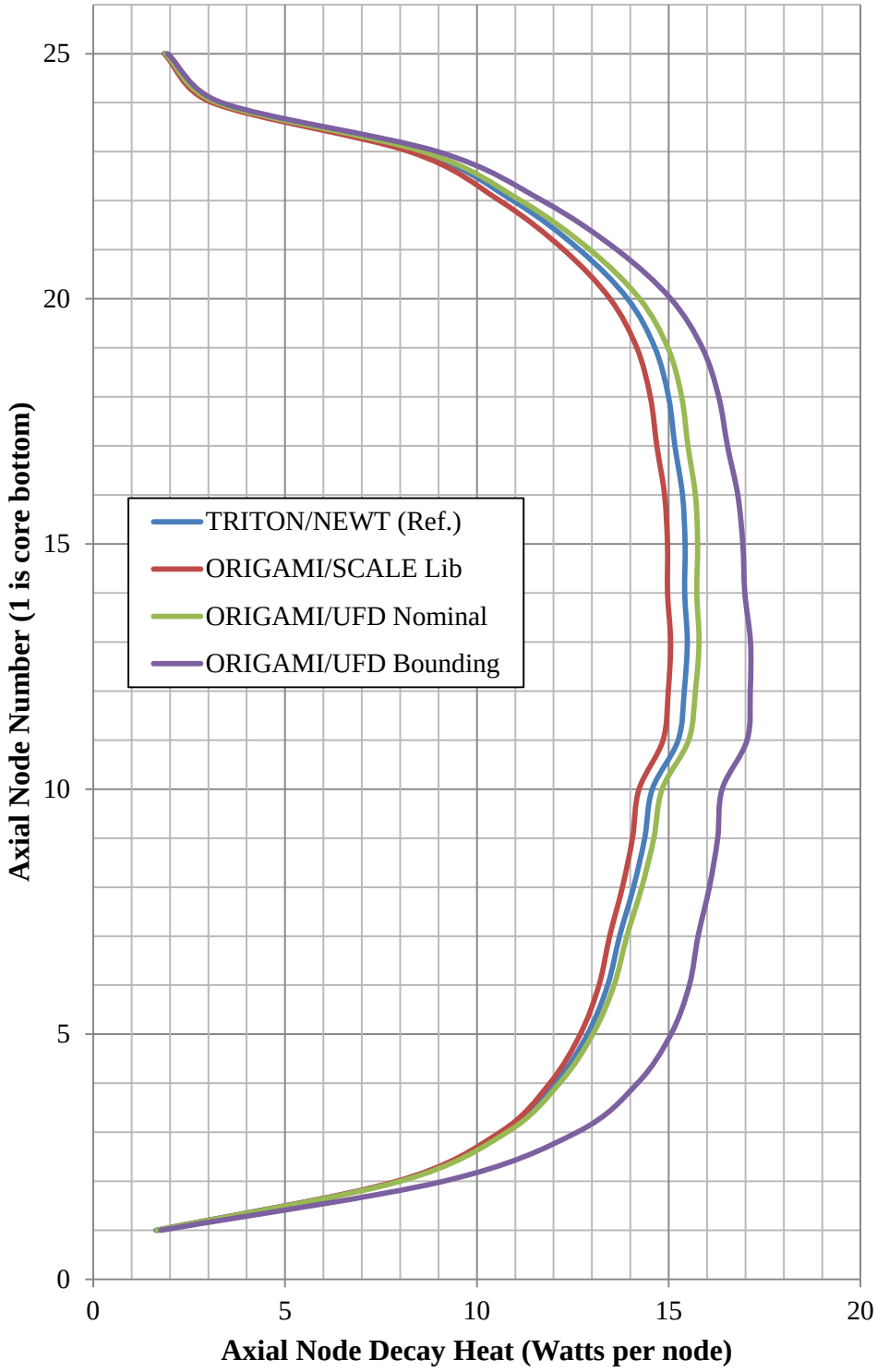


**Figure 12. Axially dependent decay heat results for HCNGS assemblyYJB732 after 5 years of postirradiation decay time**

**Table 23. Comparison of ORIGAMI and Detailed TRITON T-DEPL Calculations for HCNGS Assembly YJB732 with 50 Years of Decay Time**

| Axial Node | TRITON/NEWT (Ref.) | ORIGAMI SCALE 6.1 Library ge8×8–4 | | ORIGAMI UFD Library Nominal G4608G4B | | ORIGAMI UFD Library Bounding G4608G4B | |
|---|---|---|---|---|---|---|---|
| | Decay Heat (Watts) | Decay Heat (Watts) | Diff. from Ref. (%) | Decay Heat (Watts) | Diff. from Ref. (%) | Decay Heat (Watts) | Diff. from Ref. (%) |
| 25 | 8.85E-01 | 7.59E-01 | -14.1 | 8.62E-01 | -2.6 | 9.36E-01 | 5.8 |
| 24 | 1.49E+00 | 1.27E+00 | -14.7 | 1.42E+00 | -4.2 | 1.57E+00 | 5.4 |
| 23 | 3.40E+00 | 3.05E+00 | -10.3 | 3.24E+00 | -4.7 | 3.54E+00 | 4.1 |
| 22 | 4.31E+00 | 3.83E+00 | -11.1 | 4.08E+00 | -5.2 | 4.51E+00 | 4.6 |
| 21 | 4.91E+00 | 4.34E+00 | -11.6 | 4.65E+00 | -5.4 | 5.16E+00 | 5.1 |
| 20 | 5.33E+00 | 4.71E+00 | -11.6 | 5.04E+00 | -5.5 | 5.62E+00 | 5.5 |
| 19 | 5.56E+00 | 4.92E+00 | -11.6 | 5.25E+00 | -5.5 | 5.89E+00 | 5.9 |
| 18 | 5.67E+00 | 5.02E+00 | -11.5 | 5.35E+00 | -5.6 | 6.03E+00 | 6.4 |
| 17 | 5.71E+00 | 5.06E+00 | -11.4 | 5.39E+00 | -5.6 | 6.10E+00 | 6.9 |
| 16 | 5.76E+00 | 5.11E+00 | -11.2 | 5.43E+00 | -5.6 | 6.19E+00 | 7.5 |
| 15 | 5.76E+00 | 5.13E+00 | -10.9 | 5.44E+00 | -5.6 | 6.23E+00 | 8.2 |
| 14 | 5.73E+00 | 5.13E+00 | -10.6 | 5.42E+00 | -5.5 | 6.25E+00 | 9.0 |
| 13 | 5.73E+00 | 5.14E+00 | -10.3 | 5.42E+00 | -5.4 | 6.30E+00 | 9.9 |
| 12 | 5.69E+00 | 5.12E+00 | -9.9 | 5.38E+00 | -5.3 | 6.31E+00 | 10.9 |
| 11 | 5.60E+00 | 5.08E+00 | -9.4 | 5.31E+00 | -5.2 | 6.29E+00 | 12.2 |
| 10 | 5.35E+00 | 4.87E+00 | -8.9 | 5.08E+00 | -5.0 | 6.08E+00 | 13.6 |
| 9 | 5.26E+00 | 4.82E+00 | -8.4 | 5.00E+00 | -4.8 | 6.05E+00 | 15.1 |
| 8 | 5.13E+00 | 4.73E+00 | -7.8 | 4.90E+00 | -4.6 | 6.00E+00 | 16.8 |
| 7 | 4.98E+00 | 4.63E+00 | -7.2 | 4.77E+00 | -4.3 | 5.92E+00 | 18.7 |
| 6 | 4.85E+00 | 4.54E+00 | -6.5 | 4.66E+00 | -4.1 | 5.86E+00 | 20.8 |
| 5 | 4.66E+00 | 4.39E+00 | -5.8 | 4.48E+00 | -3.8 | 5.73E+00 | 23.1 |
| 4 | 4.36E+00 | 4.15E+00 | -5.0 | 4.21E+00 | -3.4 | 5.46E+00 | 25.2 |
| 3 | 3.92E+00 | 3.75E+00 | -4.2 | 3.80E+00 | -3.0 | 4.94E+00 | 26.1 |
| 2 | 2.99E+00 | 2.89E+00 | -3.3 | 2.92E+00 | -2.4 | 3.69E+00 | 23.3 |
| 1 | 7.24E-01 | 6.54E-01 | -9.7 | 7.17E-01 | -0.9 | 8.63E-01 | 19.2 |
| Total | 1.14E+02 | 1.03E+02 | -9.4 | 1.08E+02 | -4.9 | 1.27E+02 | 12.1 |

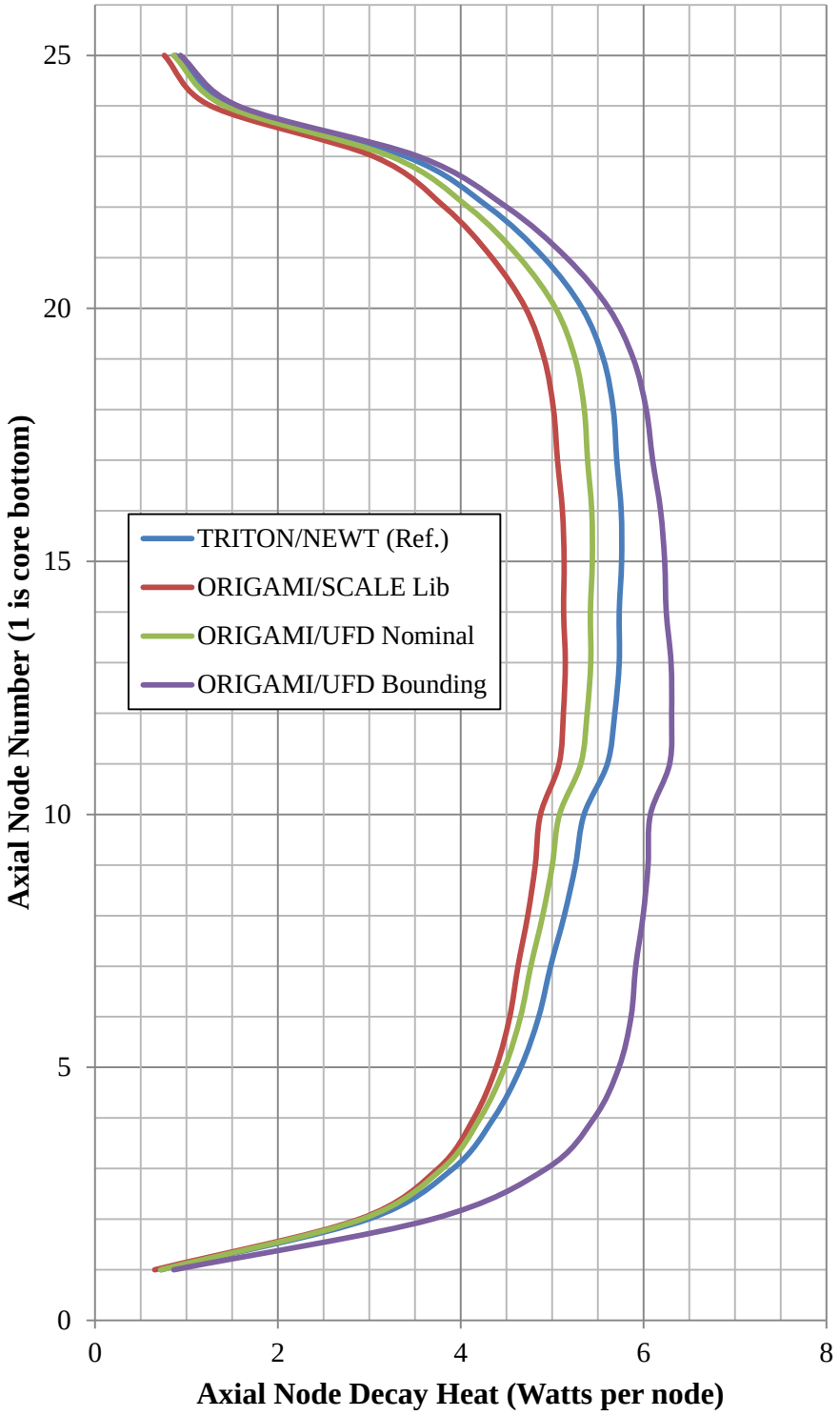


**Figure 13. Axially dependent decay heat results for HCNGS assemblyYJB732 after 50 years of postirradiation decay time**

#### *4.7.5.3 Impact of ORIGAMI Modeling Simplifications*

The last study to be presented in this report examines the impact of a couple of simplifications that one might make when using the ORIGAMI code. In the first case, the reactor depletion data for HCNGS assembly YJB732 were averaged over the axial fuel length. The average initial enrichment was 3.2292 wt % $^{235}$U, and the average power densities for the four cycles of use were 31.863, 25.669, 14.436, and 6.752 MW/MTU. Since ORIGAMI does not support moderator density variations with burnup, the overall average moderator density of 0.34139 g/cm$^3$ was used. In the second case, the lifetime average power density for the assembly of 20.0167 MW/MTU was used for the entire depletion. The original or "reference" model included axially varying enrichment, moderator density and power density. Additionally, the cycle average moderator and power densities were used. Table 24 shows the comparison of the results for a range of postirradiation cooling times.

**Table 24. Impact of ORIGAMI Modeling Simplifications**

| Decay Time (years) | 5 | | 11.8 | | 50 | |
|---|---|---|---|---|---|---|
| | Decay Heat (W/assembly) | Diff. from Ref. (%) | Decay Heat (W/assembly) | Diff. from Ref. (%) | Decay Heat (W/assembly) | Diff. from Ref. (%) |
| Reference (TRITON/NEWT) | 303.6 | - | 214.6 | - | 113.8 | - |
| Detailed ORIGAMI using data varying with axially location and modeling cycle-to-cycle variations | | | | | | |
| SCALE | 296.2 | -2.4 | 209.8 | -2.3 | 103.1 | -9.4 |
| UFD Nominal | 308.9 | 1.8 | 215.5 | 0.4 | 108.2 | -4.9 |
| UFD Bounding | 338.2 | 11.4 | 237.7 | 10.7 | 127.5 | 12.1 |
| ORIGAMI using axial average of initial enrichment, moderator and power densities. | | | | | | |
| SCALE | 288.8 | -4.9 | 205.5 | -4.3 | 102.6 | -9.8 |
| UFD Nominal | 299.8 | -1.2 | 210.2 | -2.1 | 106.7 | -6.2 |
| UFD Bounding | 330.8 | 9.0 | 233.4 | 8.8 | 126.5 | 11.2 |
| ORIGAMI using axial and assembly lifetime averages | | | | | | |
| SCALE | 321.8 | 6.0 | 209.8 | -2.2 | 103.6 | -8.9 |
| UFD Nominal | 335.5 | 10.5 | 214.8 | 0.1 | 107.7 | -5.3 |
| UFD Bounding | 370.0 | 21.9 | 238.5 | 11.1 | 127.7 | 12.2 |

The UFD bounding ORIGEN library consistently yields higher decay heat values. The axial and cycle averaging of power and moderator density appear to have significantly more effect on the decay heat for shorter decay times, where the UFD bounding library yielded a decay heat that is nearly 22% higher than the reference detailed calculation following a five-year postirradiation decay time.

# 5. CONCLUSIONS AND RECOMMENDATIONS

This report presented the results from several sensitivity studies designed to examine the impact of reactor operating parameter variations, fuel assembly design variations, and analysis techniques used on the calculated decay heat. The results from a detailed analysis of the decay heat generated by BWR assemblies in two casks at the HCNGS were used as baseline or reference results. This ensured that the sensitivity studies would be variations from real used BWR fuel. A few key observations made and conclusions reached from the studies are repeated here.

As expected, the decay heat is somewhat sensitive to modeling of BWR control blades being present. Modeling HCNGS assembly YJB732 (assembly average burnup of 37.6 GWd/MTU and cooling time of 11.8 years) with control rods present for the entire depletion, an admittedly unrealistic condition, versus modeling with no exposure to control blades resulted in about 3.4% higher decay heat. A more realistic simulation would include no more than about one cycle of control blade exposure, which would increase decay heat by about 1% compared to no control blade exposure.

The studies confirmed that decay heat generation has a small sensitivity to modeling fuel rods that include $Gd_2O_3$ because the gadolinium nuclides burn out fairly quickly and have little long lasting impact on decay heat generation.

The studies also confirmed that fuel that had an initially lower enrichment would have higher decay heat than an otherwise similar assembly used to the same assembly burnup.

Table 11 provides lists of nuclides important to decay heat generation at various postirradiation cooling times.

Some effort was expended exploring the impact of various calculational methods and approximations. Users of the SCALE TRITON sequences should be aware that use of an “addnux” value of 1 could yield significantly incorrect decay heat. This occurs primarily due to the shift of neutron flux energy and spatial distributions. In SCALE 6.1, the ORIGEN code tracks all 2,226 nuclides. The addnux variable affects only nuclides used for the flux solution in the neutron transport code and is not used by ORIGEN when it does its fuel composition calculations.

The SCALE TRITON T-DEPL sequence uses multigroup cross-section data, which includes problem-specific adjustments for resonance self-shielding. The work reported in Section 4.7.3 shows that, depending on the accuracy required, it may be necessary to calculate and use pin-specific DFs, which in one of the cases examined, increased decay heat by 1.7%.

Section 4.7.5 provided some decay heat results generated using a new SCALE sequence called ORIGAMI. This sequence uses pregenerated problem-specific ORIGEN libraries to rapidly generate used fuel compositions, decay heat, and radiation source terms. The studies performed showed that the ORIGAMI calculations can be sensitive to the ORIGEN library used, and the analyst must take care to ensure that the ORIGEN library used is appropriate for the safety analysis to be supported. Additional analysis-specific sensitivity studies should be performed to support use of ORIGAMI in support of any licensing- or safety-related work.

Table 25 provides a summary of the sensitivity study results. The reader should bear in mind that the sensitivities reported in this report are for a limited set of fuel designs and lattice variations. Information was not available for the axial distribution of the initial uranium mass. Consequently, the sensitivity studies did not include consideration of the impact of part-length fuel rods on the total and axially dependent decay heat. The results from this report should be used as indications of which parameters may be important and the direction in which decay heat values may change with parameter variations. The results should not be considered as bounding for all fuel designs and reactors.

**Table 25. Summary of Decay Heat (DH) Sensitivity Study Results**

| Parameter Studied | Description | Effect | Location |
|---|---|---|---|
| **Postirradiation Decay Time** | DH decreases with longer decay times (5 to 100 y) | -90% | Figure 5 |
| **Control Blade (CB) Use** | Modeling CB use increases DH | + 4% | Table 4 |
| | DH increases with amount of control blade use modeled | +/- 2% | Table 4 |
| | Later CB use increases DH more | +/- 2% | Table 4 |
| | DH increases more with higher burnup | 0 to +7% | Table 5 |
| | DH increases more with longer decay time | +10 to +20% | Table 5 |
| **Power Density (PD)** | DH increases with PD | +/-15% | Table 8 |
| | DH increase with PD is smaller at longer decay times | +/- 3% | Table 8 |
| Using Life-Time Average PD | Shifts burnup to later in life , increasing DH | +2% | Section 4.4 |
| **Moderator Density (MD)** | DH increases at lower MD | +/- 12% | Figure 5 |
| | DH increase with MD is smaller at longer decay times | +/- 6% | Figure 5 |
| Using Average MD for Each Axial Zone | DH increased using axially varying, life-time average MD | + 0.5% | Table 9 |
| Using Core Average MD | DH increased slightly using core average, life-time average MD | + 0.1% | Table 9 |
| **Fuel Initial Enrichment** | DH increases with lower fuel initial enrichment | +/-12% | Figs. 5 and 6 |
| | DH increase is smaller at longer decay times | +/-5% | Figs. 5 and 6 |
| **Axial DH Profile Modeling** | Using axial burnup profile to approximate axial DH distribution | -5 to +20% | Table 15 |
| **$Gd_2O_3$ Rods** | Modeling $Gd_2O_3$ rods increases DH | + 4% | Table 6 |
| | DH increase smaller with higher burnup | - 2% | Table 6 |
| | DH increase larger with longer decay times | + 4% | Table 6 |
| **Dancoff Factor (DF) Modeling** | DH increased when side, corner and interior pin DFs were used | + 2% | Table 14 |
| | DH increase was larger at lower MD (no increase at 0.75 $g/cm^3$) | 0 to +2% | Table 14 |
| **Fuel Temperature** | DH increases with fuel temperature (800K to 1100K) | + 0.3% | Table 7 |

# 6. REFERENCES

1. Code of Federal Regulations, Title 10, Part 71, *Packaging and Transportation of Radioactive Material*, January 2014.
2. Code of Federal Regulations, Title 10, Part 72, *Licensing Requirements for the Independent Storage of Spent Nuclear Fuel, High-Level Radioactive Waste, and Reactor-Related Greater than Class C Waste*, January 2014.
3. *SCALE: A Comprehensive Modeling and Simulation Suite for Nuclear Safety Analysis and Design*, ORNL/TM-2005/39, Version 6.1, Oak Ridge National Laboratory, Oak Ridge, Tennessee, June 2011. Available from Radiation Safety Information Computational Center at Oak Ridge National Laboratory as CCC-785.
4. Letter from J. M. Scaglione, ORNL, to D. E. Mueller, ORNL, on *Data for Hope Creek Decay Heat Analysis* dated August 13, 2014.
5. Letter report by G. Ilas, I. C. Gauld, and H. Liljenfeldt, *Validation of ORIGEN for Decay Heat Analysis of LWR Used Fuel*, transmitted as attachment to a letter from G. Ilas to J. M. Scaglione on September 26, 2013.
6. I. C. Gauld, G. Ilas, B. D. Murphy, and C. F. Weber, *Validation of SCALE 5 Decay Heat Predictions for LWR Spent Nuclear Fuel*, NUREG/CR-6972, ORNL/TM-2008/015, U. S. Nuclear Regulatory Commission, Oak Ridge National Laboratory, February 2010.
7. O. W. Hermann, S. M. Bowman, M. C. Brady, and C. V. Parks, *Validation of the SCALE System for PWR Spent Fuel Isotopic Composition Analyses*, ORNL/TM-12667, Oak Ridge National Laboratory, March 1995.
8. I. C. Gauld, *Strategies for Application of Isotopic Uncertainties in Burnup Credit*, NUREG/CR-6811, ORNL/TM-2001/257, U. S. Nuclear Regulatory Commission, Oak Ridge National Laboratory, June 2003.
9. G. Ilas, I. C. Gauld, F. C. Difilippo, and M. B. Emmet, *Analysis of Experimental Data for High Burnup PWR Spent Fuel Isotopic Validation-Calvert Cliffs, Takahama, and Three Mile Island Reactors*, NUREG/CR-6968, ORNL/TM-2008/071, February 2010.
10. G. Radulescu, I. C. Gauld, G. Ilas, and J. C. Wagner, *An Approach for Validating Actinide and Fission Product Burnup Credit Criticality Safety Analyses-Isotopic Composition Predictions*, NUREG/CR-7108, ORNL/TM-2011/509, U. S. Nuclear Regulatory Commission, Oak Ridge National Laboratory, April 2012.
11. D. P. Henderson, *Summary of Commercial Reactor Criticality Data for Quad Cities Unit 2*, B00000000-01717-5705-00096 REV 01, Civilian Radioactive Waste Management System M&O Contractor, September 1999.
12. D. P. Henderson, *Summary Report of Commercial Reactor Criticality Data for LaSalle Unit 1*, B00000000-01717-5705-00138 REV 00, Civilian Radioactive Waste Management System M&O Contractor, September 1999.
13. M. K. Punatar, *Summary Report of Commercial Reactor Criticality Data for Grand Gulf Unit 1*, TDR-UDC-NU-000002, Rev. 00C, Bechtel SAIC Company, LLC, September 2001.

14. I. C. Gauld and J. C. Ryman, *Nuclide Importance to Criticality Safety, Decay Heating, and Source Terms Related to Transport and Interim Storage of High-Burnup LWR Fuel*, NUREG/CR-6700, ORNL/TM-2000/284, U. S. Nuclear Regulatory Commission, Oak Ridge National Laboratory, January 2001.

15. H. Smith, J. Peterson and J.W. Hu, *Fuel Assembly Modeling for the Modeling and Simulation Toolset*, ORNL/LTR-2012-555, Rev. 1. Oak Ridge National Laboratory, October 2013.